Available online at: http://www.ijmtst.com/vol6issue05.html

International Journal for Modern Trends in Science and Technology

ISSN: 2455-3778 :: Volume: 06, Issue No: 05, May 2020

Experimental Investigation of Heat Transfer Enhancement in Solid Cylindrical & Cylindrical with Perforated Fins in Staggered & in Inline Arrangements

Hanuman Madhukar Tekale[1] | Prof.Dr.R S Pawar[2] | Prof.D A Deshmukh[3]

[1,2,3] Shreeyash College of Engineering & Technology, Aurangabad, India.

To Cite this Article

Hanuman Madhukar Tekale, Prof.Dr.R S Pawar and Prof.D A Deshmukh, "Experimental Investigation of Heat Transfer Enhancement in Solid Cylindrical & Cylindrical with Perforated Fins in Staggered & in Inline Arrangements", *International Journal for Modern Trends in Science and Technology*, Vol. 06, Issue 05, May 2020, pp.: 139-161; https://doi.org/10.46501/IJMTST060524

Article Info

Received on 02-April-2020, Revised on 28-April-2020, Accepted on 05-May-2020, Published on 17-May-2020.

ABSTRACT

In this project investigates the heat transfer enhancement in solid cylindrical and cylindrical with perforated fins in inline and staggered arrangement in rectangular channel. The channel had a cross-sectional area of 250- 100 mm2. The experiments covered the following range: Reynolds number 13,500–42,000, the clearance ratio (C/H) 0, 0.33 and 1, the inter-fin spacing ratio (Sy/D) 1.944 and 3.417. Nusselt number and Reynolds number were considered as performance parameters. Correlation equations will be developed for the heat transfer and friction factor. Computational Fluid Dynamics analysis is done by using ANSIS FLUENT 14.5 software. The Numerical and computational analysis shows that the use of the cylindrical perforated pin fins leads to heat transfer enhancement than the solid cylindrical fins. Heat transfer Enhancement varies depending on the clearance ratio and inter-fin spacing ratio. Validation of Numerical and Computational Analysis will be done.

KEYWORDS: *Heat Transfer, Cylindrical perforated Fins, Solid cylindrical fins, Staggered Arrangement, Nusselts number, Reynolds number, Fins.*

DOI: https://doi.org/10.46501/IJMTST060524

I. INTRODUCTION

E.M.Sparrow [1] Laminar fully developed flow and heat transfer have been analyzed for a duct in which there ore cross-sectional non uniformities. The non uniformity consists of a span wise-periodic array of rectangular protuberances that extend into the flow cross section from an otherwise plane wall. The other bounding wall of the flow cross section is plane and smooth (no protuberances). To attain solutions with a minimum number of parameters, the general problem of heating at both walls is broken down into two sub problems, in each of which only one of the two walls is heated. Extensive numerical solutions were carried out for each of the sub problems, and the superposition procedure by which these results are used for the general problem is described. The finite-difference formulation was facilitated by the use of two-nodded control volumes deployed adjacent to the boundaries of the solution domain.

D.E.Metzger et al. [2] The effects of array configuration and pin-endwall fillet on the heat transfer and pressure drop of short pin-fin arrays are investigated experimentally. The pin-fm element with endwall-fillet, typical in actual turbine cooling applications is modeled by a spool-like cylinder. The arrays studied include an in-line and a staggered array, each having 7 rows of 5 pins. These arrays have the same geometric parameters, i.e. H/D = 1, S/D = X/D = 2.5, and the Reynolds number ranging from 5×10^3 to 3×10^4. One of the present results shows that the staggered array always has a higher array-averaged mass transfer coefficient than its in-line counterpart. However, the pressure drop for the staggered array is higher compared to the in-line configuration. These trends are unaffected by the existence of the pin-endwall fillet. Another significant finding is that an array with pin- endwall fillet generally produces lower heat transfer coefficient and higher pressure drop than that without endwall-fillet. This leads to the conclusion that pin-endwall fillet is undesirable for heat transfer augmentation. In addition, naive use of the heat transfer results obtained with perfectly circular cylinders tends to overestimate the pin-fin cooling capability in the actual turbine. The effects of end wall-fillet on the array heat transfer and pressure drop are much more pronounced for the staggered array than for the in-line array; however, they diminish as the Reynolds number increases. Investigated the effects of pin-fin shape and array orientation on the heat transfer and the pressure loss in pin-fin arrays. According to their results, the use of cylindrical pin-fins with an array orientation between staggered and in-line can sometimes promote the heat transfer, while substantially reducing pressure. When oblong pin-fins are used, heat transfer increases of around 20% over the circular pin-fins were measured, but these increases were offset by increases in the pressure loss of around 100%. Their estimate indicated that the pin-fin surface coefficients were approximately double the end wall values.

G.J.Vanfossen and B.A. Brigham [3]Studied the heat transfer by short pin-fins in staggered arrangements. According to their results, longer pin-fin in staggered arrangement. According to their results longer pin-fin (H/d=4) transfer more heat than shorter fin (H/d=0.5 and 2) and the array- averaged heat transfer with eight rows of pin-fins slightly exceeds that with only four rows. Their result also established that the average heat transfer coefficient on the fin surfaces is around 35% larger than that on the wall end.

R. Karthikeyan , R. Rathnasamy [4] studied the heat transfer and friction characteristics of convective heat transfer through a rectangular channel with cylindrical and square cross-section pin-fins attached over a rectangular duralumin flat surface. The pin-fins were arranged in in-line and a staggered manner. Various clearance ratios (C/H=0.0, 0.5&1.0) and inter-fin distance ratios (Sy/d and Sx/d) were used. The experiments are conducted for various mass flow rate of air (Re ranges from 2000-25000). The experimental results showed that the use of square cross-section pin-fins may lead to an advantage on the basis of heat transfer enhancement. For higher thermal performance, lower inter fin distance ratio and clearance ratio and comparatively lower Reynolds numbers should be preferred for in-line and staggered arrangement. The results of the in-line configurations were also compared with the results of the staggered arrangements for the two types of pin-fins and the average Nusselt number increased with increasing Reynolds number the average Nusselt number increased with decreasing clearance ratio and inter-fin distance ratio. For a given Reynolds number, the pin-fin array with smaller inters fin distance gives higher performance than those with higher inter fin distances. The friction factor increased with decreasing clearance ratio and inter-fin distance ratio. The staggered pin-fin array significantly enhanced heat transfer as a result turbulence at the expense of higher pressure drop in the wind tunnel. Square pin-fin array performance is slightly higher than the cylindrical array with the penalty of pressure drop.

O.N. Sara et al. [5] reported heat-transfer enhancement and the corresponding pressure drop over a flat surface in a channel flow due to perforated rectangular cross-sectional blocks attached on its surface. The channel had a cross-sectional area of 80×160 mm^2 with blocks 10×25 mm^2. The experiments covered the following range: Reynolds number (Re) 6670-40 000, the hole inclination angle (0) 0-45°, the perforation open-area ratio (F) 0.05-0.15, the diameter of the perforations (D) 2.5-8.0 mm, and the number of the blocks (Nb) 2-7 (giving the ratio of the distance between the blocks to the channel hydraulic diameter (Sx/Dc) 1.407-0.309). The blocks were transverse to the main flow. It was observed that the heat-transfer enhancement

increased with increasing s and D and decreasing Sx/Dc and Re. The pressure drop was not affected while it decreased with increasing D, Re, Sx/Dc, and s. Correlation equations were developed for the average Nusselt number (Nu) and the friction factor (f). Performance analysis indicated that the solid blocks could lead to energy loses up to 20% despite significantly enhanced heat-transfer due to the increased surface area. reported another way to improve heat transfer rate is to employ attachments with (i) perforations, (ii) a certain degree of porosity or (iii) slots which allow the flow to go through the blocks. In the case of perforated attachments, the improvement in the flow (thus the enhancement in the heat transfer) is brought about by the multiple jet-like flows through the perforations. Jet flows are associated with high overall and localized transport characteristics due to not only increased shear induced mixing (turbulence) at the edges of the jet as the flow progresses downstream but also high velocities and turbulence (depending on the distance from the jet exit) in the impact zone. Thus, the aim of this study is also to determine heat transfer and friction factor characteristics of the perforated staggered cylindrical fins. The heat transfer enhancement is achieved at the expense of the increased pressure drop. For many practical applications it may thus be necessary to determine the economic benefit for the heat transfer.

R.F. Babus'Haq et al. [6] reported that the optimal ratio of the inter-fin pitch to the pin fin diameter in the transverse direction was 2.04 for all pin-fin Systems. However, the optimal ratios in the longitudinal direction were 1.63, 1.71 and 1.95 for polytetrafluoroethene pin-fins, mild-steel pin-fins and duralumin pin-fins respectively.

Tahat, M. & Kodah, Z. H. & Jarrah, B. A. & Probert, S. D [7] Steady-state heat-transfers from pin-fin arrays have been investigated experimentally for staggered and in-line arrangements of the pin fins, which were orthogonal to the mean air-flow. For the applied conditions, the optimal spacings of the fins in the span-wise and stream-wise directions have been determined. The dependences of the Nusselt number upon the Reynolds number and pin-fin pitch (in both directions) have been deduced.

Giovanni Tanda [8] studied heat transfer and pressure drop experiments were performed for a rectangular channel equipped with arrays of diamond-shaped elements. Both in-line and staggered fin arrays were considered, for values of the longitudinal and transverse spacing's, relative to the diamond side, from 4 to 8 and from 4 to 8.5, respectively. The height-to-side ratio of the diamonds was 4.0. Liquid crystal thermo graphs was used to determine the heat transfer coefficients on the surface of the channel (end wall) on which the fins were mounted. Local variations in heat transfer coefficients induced by the arrangements of the diamond-shaped elements were measured and discussed. Correlations giving the average Nusselt number for each configuration as a function of the Reynolds number were developed. Thermal performance comparisons with data for a rectangular channel without fins showed that the presence of the diamond-shaped elements enhanced heat transfer by a factor of up to 4.4 for equal mass flow rate and by a factor of up to 1.65 for equal pumping power.

Tzer-Ming Jeng, Sheng-Chung Tzeng [9] studied the pressure drop and heat transfer of a square pin-fin array in a rectangular channel. The variable parameters are the relative longitudinal pitch (XL = 1.5, 2, 2.8), the relative The performance of the square pin-fins as the cooling devices is compared with that of the circular pin-fins. The result shows that The in-line square pin-fin array has smaller pressure drop than the in-line circular pin-fin array at high XT (XT = 2.0 or 2.8) but an equivalent (or even slightly higher) pressure drop at low XT (such as XT = 1.5). Additionally, the staggered square pin-fin array has the largest pressure drop of the three pin fin arrays (in-line circular pin-fins, in-line square pin-fins and staggered square pin-fins). Most in-line square pin-fin arrays have poorer heat transfer than an in-line circular pin-fin array, but a few, as when XL = 2.8, exhibit excellent heat transfer at high Reynolds number. For instance, when XL = 2.8, XT = 1.5 and Red (Umax/U) = 12,500, the fin Nusselt number (Nud) of square pin-fins is around 40% higher than that of circular pin-fins. Moreover, when Red(Umax/U) exceeds 6000, the Nusselt number of the staggered square pin-fin array generally exceeds that of the in-line circular pin- fin array. When XT = 1.5, XL = 2.8 and Red(Umax/U) = 12,500, the heat transfer of the staggered square pin- fin array is around 20% higher than that of the in-line circular pin-fin array. The optimal inter-fin pitches are determined by the largest Nusselt number at a given pumping power. The optimal inter-fin pitches of in-line square pin fin arrays are XT = 2 and XL = 1.5, its Nu_d is around 20% higher than that of the in-line circular pin-fin array. However, the staggered square pin-fin array performs best at XT = 1.5 and

XL = 1.5. Furthermore, at XT = 1.5 and XL = 1.5 and when fdRe3d exceeds 2.5 _ 1010, the Nu_ d of the staggered square pin-fin array exceeds that of the in-line circular pin fin array; and when fdRe3 d ¼ 2:0 _ 1011, the Nu_d of the staggered square pin-fin array is 25% higher than that of the in-line circular pin-fin array. transverse pitch (XT = 1.5, 2, 2.8) and the arrangement (in-line or staggered). Compared with the open articles, the present relative pitches are smaller and independently variable.

Bayram Sahin, Alparslan Demir [10] studied the heat transfer enhancement and the corresponding pressure drop over a flat surface equipped with square cross-sectional perforated pin fins in a rectangular channel. The channel had a cross-sectional area of 100–250 mm2. The experiments covered the following range: Reynolds number 13,500–42,000, the clearance ratio (C/H) 0, 0.33 and 1, the inter-fin spacing ratio (Sy/D) 1.208, 1.524, 1.944 and 3.417. Correlation equations were developed for the heat transfer, friction factor and enhancement efficiency. The experimental results showed that the use of the square pin fins may lead to heat transfer enhancement. Enhancement efficiencies varied between 1.1 and 1.9 depending on the clearance ratio and inter- fin spacing ratio. Both lower clearance ratio and lower inter-fin spacing ratio and comparatively lower Reynolds numbers are suggested for higher thermal performance. In this study, the overall heat transfer, friction factor and the effect of the various design parameters on the heat transfer and friction factor for the heat exchanger equipped with square cross-sectional perforated pin fins were investigated experimentally. The effects of the flow and geometrical parameters on the heat transfer and friction characteristics were determined, and the enhancement efficiency correlations have been obtained The average Nusselt number calculated on the basis of projected area increased with decreasing clearance ratio and inter-fin spacing ratio. The friction factor increased with decreasing clearance ratio and inter-fin distance ratio. Enhancement efficiencies increased with decreasing Reynolds number. Therefore, relatively lower Reynolds number led to an improvement in the heat transfer performance. The most important parameters affecting the heat transfer are the Reynolds number, fin spaces (pitch) and fin height. Heat transfer can be successfully improved by controlling these parameters. The maximum heat transfer rate was observed at 42,000 Reynolds number, 3.417 Sy/D and 50 mm fin height. The most effective parameter on the friction factor was found to be fin height. The minimum friction factor was observed at 50 mm. fin height, 42,000 Reynolds number and 3.417 pitch. When all the goals were taken into account together, the trade off among goals was considered and the optimum results were obtained at 42,000 Reynolds number, 50 mm fin height and 3.417 Sy/D pitch. M.R Shaeri, M.Yaghoubi [11] Investigated analysis of turbulent convection heat transfer from an array of perforated fins, numerical investigation is made for three dimensional fluid flow and convective heat transfer from an array solid and perforated fin that are mounted on flat plate, sometimes an image may contain text embedded on to it. Detecting and recognizing these characters can be very important, and removing these is important in the context of removing indirect advertisements, and for aesthetic reasons. perforation such as small channels with square cross section are arranged stream wise along the fins length and their number varied from 1 to 3 flow and heat transfer characteristics are presented by Reynolds number from 2x104 and 4x104 based on the fin length of previous investigation and good agreement were observed result show that fins with longitudinal pores have unmark able heat transfer enhancement in addition to the consider reduction in weight by comparison with solid fins. Jnana Ranjan Senapati and Sukanta Kumar Dash and Subhranshu Roy [12]

Numerical convection heat transfer from an annular finned horizontal cylinder with different eccentricity has been studied numerically in the this work. This paper present numerical investigation is able to capture a complete picture of natural convection over a horizontal cylinder with fins of different eccentricity. In present conjugate heat transfer study of annular finned horizontal cylinder annular disc fins can be design for the

Purpose to increase the heat transfer rate significantly with marginal loss in the heat transfer with respect to the concentric annular fins. Tamir K. Ibrahim,and Marwah N. Mohammed,and Mohammed kamil Mohammed,and Najafi,and Nor azwadi Che Sidik,and firdaus Basrawi,and Ahamed n, Abdalla &and S.S. Hoseini [13]

This paper investigates the effect of perforation shape on the heat transfer of perforated fins. This types of heatexchanger used in heat sink with the perforated fins under the forced convection heat transfer to determine the performance for each

perforation shape between circular. Cylindrical, rectangular triangular, and also with the non perforated fins. The experimental result compare between perforations shape and the heat transfer coefficient to clarify the best perforation shape for the plate heat sink after studied experimentally and numerically using CFD. The difference between experimental & numerical is reported about 8 % & 9% for temperature distribution when power supplied is 150 W 100W respectively. The higher temperature difference of the fins is with the circular. Perforation shape which is 51.29% when compared with at the tip of the fins with the temperature at the heat collector followed by the rectangular perforation shape with 45.57 then followed by the rectangular perforation shape by 42.28% then lastly the non perforated fins by 35.82%. The perforation of the fins shows significant effect on the performance of force

II. Research Gap

The researchers done before on heat transfer enhancements in various types of geometries of fins by taking various parameters like Reynolds number, prandtl number, Nusselt number and taking various inter fin spacing ratio, clearance ratio etc. This project investigates the heat transfer enhancement in solid cylindrical & perforated cylindrical fins in inline and staggered arrangement in rectangular channel. The channel had a cross-sectional area of 250-100 mm2. The experiments covered the following range: Reynolds number 13,500–42,000, the clearance ratio (C/H) 0, 0.33 and 1, the inter-fin spacing ratio (Sy/D) 1.944 and 3.417. Nusselt number and Reynolds number were considered as performance parameters. Correlation equations will be developed for the heat transfer and friction factor. Computational Fluid Dynamics analysis is done by using ANSIS FLUENT14.5 software. The Numerical and computational analysis shows that the use of the cylindrical perforated pin fins leads to heat transfer enhancement than the solid cylindrical fins. Heat transfer Enhancement varies depending on the clearance ratio and inter-fin spacing ratio. Validation of Numerical and Computational Analysis will be done.

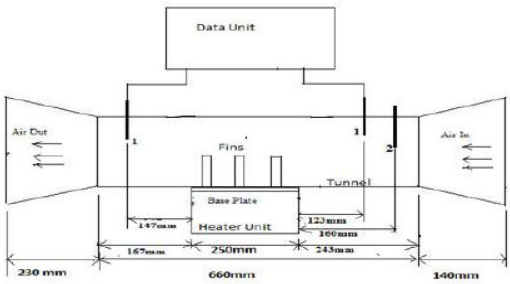

. Fig.(2) Experimental Set-up

The experimental set-up consisting of the following parts

1) Main Duct (Tunnel)
2) Heater Unit
3) Base Plate
4) Data Unit

Main Duct (Tunnel):

Tunnel constructed of wood of 20 mm thickness, had an internal cross-section of 250 mm Width and 100 mm the total length of the channel is 1000 mm. It will be operated in force draught mode by the blower of 0.5 H.P., 0 to 13000 rpm, 220W, 1.8Kg, variable speed 1 to 6 and it is fitted at 120cm away from the entry of the tunnel positioned horizontally and flow of air is controlled by the flow control valve mounted just after the blower. It has a convergent and divergent section at both ends having the inclination of 30°. A Matrix anemometer is mounted in a tunnel to measure the mean inlet velocities of the air flow entering to the test Section the range of this anemometer is 0 to 40m/sec.

The Reynolds number range used in this experiment was 13,500–42,000, which is based on the hydraulic diameter of the channel over the test section (Dh) and the average velocity (U)

The inlet and outlet temperature of the air stream and temperature of base plate will be measured by RTD Sensors having a range of 0°C to 450°Cwhich mounted in wind tunnel.

Figure.5 Main Duct

Heater Unit:

Heater Unit (test section) has a cross-section of 250 mm x 250 mm square; the heating unit mainly consisted of an electrical heater placed between two M.S. Plate having the same Dimension of base

plate, a two firebrick of 250mm x220 mm. Dimensions of the electrical Heater placed on the firebrick is 250 mm x 250 mm. The heater output has a power of 2000 W at 220V and a current of 10 Amp.

BASE PLATE:

It consist of square plate at base having the dimension 250mm x 250 mm, thickness is 6mm and The pin fins and base plate made of the same material i.e. Aluminum because of the Considerations of conductivity, mach inability and cost. The fins have a circular cross section of 15 mm x15 mm and are attached on the upper surface of the base plate as shown in Fig. 3. Circular pin fins with different lengths, constant C/H (Clearance ratio) values of 0 and are perforated at the 17 mm from bottom tip of those by an 8 mm diameter drill bit. The pin fins are fixed uniformly on the base plate with a constant spacing between the slantwise directions of 18.125 mm, with different spacing between the pin fins in the stream wise direction. The spacing ratios of the pin fins in the stream wise direction (Sy/D) were 1.944 and 3.417 mm for both Staggered arrangement and Inline arrangement, giving different numbers of the pin fins on the base plate. It is well-known fact that if the inter-fin spacing in the span wise direction.

Data Unit

It consist of various indicating devices which indicates the reading taken by the various Component like RTD sensors, pressure gauges, Anemometer There are three Temperatures Indicator which shows reading taken by the RTD Sensors in the range 0°c to 450 °c among This two gives inlet and out temperature of air and one gives temperature of base plate There is one temperature contractor which can maintain the temperature of base plate it will not Allow to exceed the temperature of base plate above desired values. Two pressure gauges are Mounted on the data unit which shows the inlet and outlet pressure of air in the range of 0 to 150 kg/cm² inside the tunnel. Inlet flow rate of air is indicated by velocity indicator using Anemometer. MCB Hedger switches are mounted to cut off the power supply in case any Short circuit

Experimental Procedure

First of all make all the necessary attachment to wooden tunnel required for Experimental set-up attachment of data unit, attachment of blower unit, attachment of heater unit

- Keep the aluminum base plate of required dimensions on heater unit.
- Move the heater unit upward by rotating the screw jack.
- Switch on the RTD sensors of inlet, outlet and base
- plate temperature indicator and Check whether it is
- Properly functioning or not.

Measure the room temperature by anemometer by For Perforated Fins Sy/D=3.417 i.e. No. of Fins on one base plate=11 No.

- Changing the function of it to Temperature mode.

Switch on the heater, as soon as base plate temperature reached up to 100°C, the Temperature controller of RTD sensors comes in Operation and it will cut off the Power supply of heater. Once the temperature of base plate reduced up to 99°C again Temperature controller of RTD sensors comes in operation and start the power supply. of heater and cycle gets repeat.

- Now switch on the blower and measure the velocity of inlet air by using digital Anemometer. Make the inlet air velocity constant at required velocity by regulating the speed of blower i.e. 2m/s, 3m/s, 4m/s, and 5m/s.
- Now air will pass over heated base plate through tunnel
- Measure the outlet temperature of outgoing warm air

  Now due to forced convection the temperature of base plate falls below 100°C. As Soon as the temperature of base plate falls.
- Below the 100°C heater unit will start Heating the base plate to achieve the constant 100°C temperature by supplying Constant electrical input as the air is continuously flowing over the base plate heat get Transferred from it to the flowing air. Thus the temperature of base plate falls Continuously and take the temperature readings of base plate after 90 seconds of air

  Flow. The duration of air flow is constant for all types of base plate mentioned above.
- Similarly, repeat the same procedure for velocity 3m/s, 4m/s, and 5m/s and take the Similar readings.

Details of Dimension and no.of base plate & fins

Sr.No	Particulars	Size(mm)	Quantity
1	Base plate (Without fins)	250x250	01
2	Base plate with fins	250x250	08
3	Perforated	100	85

	fins		
4	Solid Fins	100	85

Sr. No.	Velocity ($^m/_s$)	Surface Temp. (°c)(T_s)	Inlet Temp.(°c) (T_{in})	Outlet Temp.(°c) (T_{out})
1	2	100	32	43
2	3	100	33	42
3	4	100	33	41
4	5	100	32	39

Sr. No.	Velocity ($^m/_s$)	Surface Temp. (°c)(T_s)	Inlet Temp.(°c) (T_{in})	Outlet Temp.(°c) (T_{out})
1	2	100	32	44
2	3	100	32	41
3	4	100	32	41
4	5	100	32	40

III. Details of dimension & No. of base plat

Performance Analysis

Experimental Observations

Sr. No.	Velocity ($^m/_s$)	Surface Temp. (°c)(T_s)	Inlet Temp.(°c) (T_{in})	Outlet Temp.(°c) (T_{out})
1	2	100	31	39
2	3	100	31	38
3	4	100	32	38
4	5	100	32	37

After conducting the experiment the following reading are obtained for the respective conditions

For Constant C/H=0 i.e. Fin Height=100mm
Voltage=230V, Current=6.5 amp
For Staggered Arrangement (Perforated)

1) For Perforated Fins Sy/D=1.944 i.e. No. of Fins on one base plate=18 No

Table 4.1.1 For Perforated Fins Sy/D=1.944 i.e. No. of Fins on one base plate=18 No

2) For Perforated Fins Sy/D=3.417 i.e. No. of Fins on one base plate=11 No

Table 4.1.2 For Perforated Fins Sy/D=3.417 i.e. No. of Fins on one base plate=11 No

For Staggered Arrangement (Solid)

3)For Solid Fins Sy/D=1.944 i.e. No. of Fins on one base plate=18 No.

Table 4.1.3 For Solid Fins Sy/D=1.944 i.e. No. of Fins on one base plate=18 No.

4)For Solid Fins Sy/D=3.417 i.e. No. of Fins on one base plate=11 No.

Table 4.1.4 For Solid Fins Sy/D=3.417 i.e. No. of Fins on one base plate=11 No.

Sr. No.	Velocity ($^m/_s$)	Surface Temp. (°c)(T_s)	Inlet Temp.(°c) (T_{in})	Outlet Temp.(°c) (T_{out})
1	2	100	33	40
2	3	100	33	39
3	4	100	32	38
4	5	100	32	36

For Inline Arrangement (Perforated)

1) For Perforated Fins Sy/D=1.944
i.e. No. of Fins on one base plate=35 No.
Table 4.2.1 For Perforated Fins Sy/D=1.944 i.e. No. of Fins on one base plate=35 No.

Sr. No.	Velocity ($^m/_s$)	Surface Temp. (°c)(T_s)	Inlet Temp.(°c) (T_{in})	Outlet Temp.(°c) (T_{out})
1	2	100	32	42
2	3	100	33	40
3	4	100	32	40
4	5	100	32	38

2)For Perforated Fins Sy/D=3.417
i.e. No.of Fins on one base plate=21 No.Table 4.2.2 For Perforated Fins Sy/D=3.417 i.e. No. of Fins on one base plate=21 No.

Sr. No.	Velocity ($^m/_s$)	Surface Temp. (°c)(T_s)	Inlet Temp.(°c) (T_{in})	Outlet Temp.(°c) (T_{out})
1	2	100	33	40
2	3	100	32	38
3	4	100	32	37
4	5	100	32	37

For Inline Arrangement (Solid)

3)For Solid Fins Sy/D=1.944
i.e. No. of Fins on one base plate=35 No.Table 4.2.3 For Solid Fins Sy/D=1.944i.e. No. of Fins on one base plate=35 No.

Sr. No.	Velocity ($^m/_s$)	Surface Temp. (°c)(T_s)	Inlet Temp.(°c) (T_{in})	Outlet Temp.(°c) (T_{out})

1	2	100	33	42
2	3	100	32	40
3	4	100	32	39
4	5	100	32	37

4))For Solid Fins Sy/D=3.417 i.e. No. of Fins on one base plate=21 No.

Table 4.2.4 For Solid Fins Sy/D=3.417 i.e. No. of Fins on one base plate=21 No.

Sr. No.	Velocity (m/s)	Surface Temp. (°c)(T_s)	Inlet Temp.(°c) (T_{in})	Outlet Temp.(°c) (T_{out})
1	2	100	32	38
2	3	100	32	37
3	4	100	32	37
4	5	100	32	36

For Smooth Duct i.e. Base Plate without Fins

Table 4.3 For Smooth Duct i.e. Base Plate without Fins

Sr. No.	Velocity (m/s)	Surface Temp. (°c)(T_s)	Inlet Temp.(°c) (T_{in})	Outlet Temp.(°c) (T_{out})
1	2	100	32	33
2	3	100	32	33
3	4	100	32	33
4	5	100	32	33

4.2 Sample calculations for Experimental Analysis

For Sample calculation Table 1 is taken and air velocity = 2m/s

For Perforated Fins Sy/D=1.944 i.e. No. of Fins on one base plate=18 No

For Perforated Fins, C/H=0, i.e. Fin height=100mm

Sr. No.	Velocity (m/s)	Surface Temp. (°c)(T_s)	Inlet Temp.(°c) (T_{in})	Outlet Temp.(°c) (T_{out})
1	2	100	32	44
2	3	100	32	41
3	4	100	32	41
4	5	100	32	40

The convective heat transfer rate Q convection from electrically heated test surface is calculated by using

$$Q_{conv.} = Q_{elect.} - Q_{cond.} - Q_{rad.}$$

Where 'Q' indicates the heat transfer rate in which subscripts conv, elect, cond and rad denotes convection, electrical, conduction and radiation, respectively. In similar studies, investigators reported that total radiative heat loss from a similar test surface would be about 0.5% of the total electrical heat input. The conductive heat losses through the sidewalls can be neglected in comparison to those through the bottom surface of the test section. Therefore the electrical heat input is calculated from the electrical potential and current supplied to the surface.

$$Q_{conv} = Q_{elect}$$
$$Q_{elect.} = I^2 \times R$$

As per experimental data I=6.5 amp and V=230V

Hence by Ohm's Law

$$R = \frac{V}{I} = \frac{230}{6.5} = 35.38\ \Omega$$

Therefore,

$$Q_{elect.} = I^2 \times R = 6.5^2 \times 35.38 = 1495\ W$$

As $Q_{conv.} = Q_{elect.} = 1495$ W

Now $Q_{conv.} = h_{av} A_s \left[T_s - \left(\frac{T_{out}+T_{in}}{2}\right)\right]$

Hence, the average convective heat transfer coefficient have could be deduced via

$$h_{av} = \frac{Q_{conv.}}{A_s \left[T_s - \left(\frac{T_{out}+T_{in}}{2}\right)\right]}$$

Total area (As) = Projected area + Total surface area contribution from the blocks

$$A_s = WL + [\pi DH - 2\pi ab]N_p + [(2\pi r^2 + 2\pi rD) - 2\pi ab]N_p$$

A_s=250x250 + [3.14x15x100 – 2x3.14x4x4.8]18 + [(2x3.14x4^2+ 2x3.14x4x15) - 2x3.14x4x4.8] 18

$A_s = 0.1515 m^2$

Heat Transfer Coefficient $h_{av1} = \frac{1495}{0.1515\left[100 - \left(\frac{44+32}{2}\right)\right]}$

h_{av2} = 159.16 w/m^2 °c

Reynolds No. $R_e = \frac{D_h U}{\nu}$

$$Reynolds\ No.\ R_e = \frac{0.14286 \times 2}{16.83 \times 10^{-6}}$$

$$Reynolds\ No.\ R_e = 16976.82$$

4.2.1 Calculation for Heat Transfer

In order to have basis for the evaluation of the effects of the fins, the average nusselt number (Nus) for the smooth surface (without fins) and Nu with fins will be correlated as function of Re and Pr as follows and suffix 2 represent the velocity at 2m/s.

Nu_s For Smooth Duct (Without Fin) $Nu_{s2} = 0.077 Re^{0.716} Pr^{1/3}$

$$Nu_{s2} = 0.077 \times 16976.82^{0.716} \times 0.7^{1/3}$$

$$Nu_{s2} = 69.58$$

$Nu\ (with\ fin) Nu_2 = 45.99 Re^{0.396} (1 + C/H)^{-0.608} (S_y/D)^{-0.522} Pr^{1/3}$

$$Nu\ (with\ fin) Nu_2 = 45.99(16976.82)^{0.396}(1 + 0)^{-0.608}(1.944)^{-0.522} 0.7^{1/3}$$

$$Nu_2 = 1365.69$$

This equations are valid for the experimental conditions of 13,500 ≤ Re ≥ 42,000, 1.944 < Sy/D < 3.417, C/H = 0 and Pr = 0.7 by using this equation the Nu/Nus and Re will be determine for perforated fins for constant C/H ratio i.e. C/H=0 and for different Sy/D ratios i.e. Sy/D=1.944, Sy/D=3.417 The same will be find out for solid fins and the comparative graph between Nu/Nus and Re for perforated fins and solid fins will be plot

$$\frac{Nu_2}{Nu_{s2}} = 19.62$$

4.2.2 Calculation for Friction Factor

The pressure drops in the tunnel without fins is so small that they could not be measured by the Manometer. This resulted from smaller length of the test section and smaller roughness of the duct. The experimental pressure drops over the test section in the finned duct will be measured under the heated flow conditions. These measurements will be converted to the friction factor '*F*' Using the experimental results, f was correlated as a function of the duct Reynolds number, Re, and geometrical parameters. The resulting equation is

$$F_2 = 2.4 Re^{-0.0836} (1 + C/H)^{-0.805} (S_y/D)^{-0.0814}$$

$$F_2 = 2.4 \times 16976.82^{-0.0836} (1+0)^{-0.0836} (1.944)^{-0.0814}$$

$$F_2 = 1.0061$$

Similarly, we can calculate all above parameters for Different velocities like V=3, V=4, V= 5.

After doing calculations for Nusselt Number and Friction factor for all 9 tables, following values are obtained and it is summarized in the tabular form as follows.

Table No. 4.7

Values for Staggered Arrangement (C/H = 0)

			at V=2 m/s	at V=3 m/s	at V=4 m/s	at V=5 m/s	at V=2 m/s	at V=3 m/s	at V=4 m/s	at V=5 m/s	at V=2 m/s	at V=3 m/s	at V=4 m/s	at V=5 m/s
	Sy/D	(As) in m^2	Nu/ Nus2	Nu/ Nus3	Nu/ Nus4	Nu/ Nus5	Re_2	Re_3	Re_4	Re_5	F_2	F_3	F_4	F_5
Perforated	**1.944**	0.1515	19.62	17.11	15.51	14.61	16976.82	25678.84	34238.46	42926.68	1.0061	0.9729	0.9427	0.9319
	3.417	0.1169	14.95	12.91	11.70	10.88	17264.04	25974.54	34528.09	43290.9	0.9606	0.9223	0.9015	0.8855
Solid	**1.944**	0.1473	19.23	16.63	15.13	14.12	17027.4	25586.86	34156.6	43030.12	1.0042	0.9711	0.9419	0.9308
	3.417	0.1143	14.41	12.63	11.43	10.70	17119.23	25756	34528.09	43422.49	0.9592	0.9211	0.901	0.8815

Table.No.4.8
Values for Inline Arrangement (C/H = 0)

			at V=2 m/s	at V=3 m/s	at V=4 m/s	at V=5 m/s	at V=2 m/s	at V=3 m/s	at V=4 m/s	at V=5 m/s	at V=2 m/s	at V=3 m/s	at V=4 m/s	at V=5 m/s
	Sy/ D	(As) in m^2	Nu/ Nus2	Nu/ Nus3	Nu/ Nus4	Nu/ Nus5	Re_2	Re_3	Re_4	Re_5	F_2	F_3	F_4	F_5
Perforated	**1.944**	0.2357	18.75	16.64	15.02	13.98	16836.77	25255.15	33673.54	42091.92	1.009	0.9792	0.9511	0.9385
	3.417	0.1664	13.89	12.24	11.09	10.32	17108.98	25896.07	34632.72	43290.9	0.9693	0.9285	0.9072	0.8895
Solid	**1.944**	0.2274	18.18	16.36	14.67	13.63	16976.82	25756	34424.09	43160.12	1.082	0.9766	0.9483	0.9365
	3.417	0.1614	13.35	12.05	10.83	10.11	17264.04	25974.54	34632.72	43406.66	0.9676	0.9263	0.9049	0.8883

Result of Experimental Analysis

From the above calculations the actual values are obtained for nusselt number and friction factor on the basis of these values graphs are plot between Nusselt No. and Reynolds No., Friction factor and Reynolds No

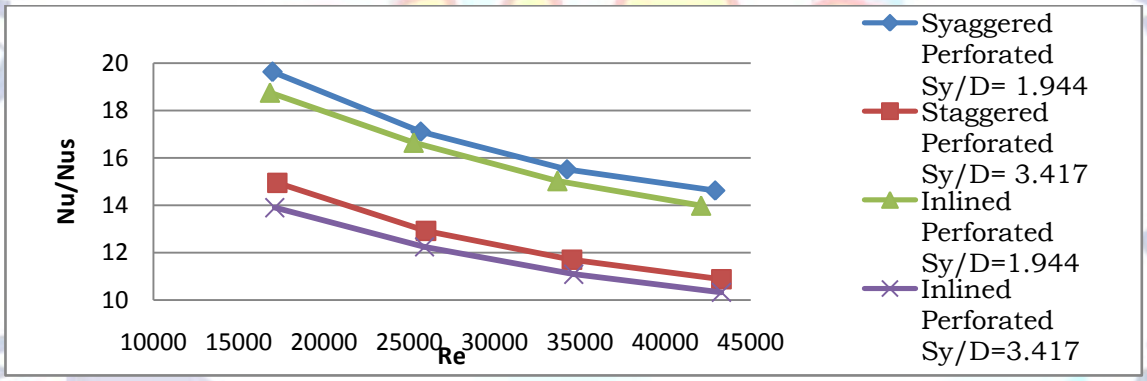

Fig:-4.3.1 Variation of Nu/Nus with Reynolds No. (Re) for various inter-fin spacing ratio (Sy/D) for Staggered Perforated & Inline Perforated arrangement

Fig:- 4.3.2Variation of Nu/Nus with Reynolds No. (Re) for various inter-fin spacing ratio (Sy/D) for Staggered Solid & Inline Solid arrangement

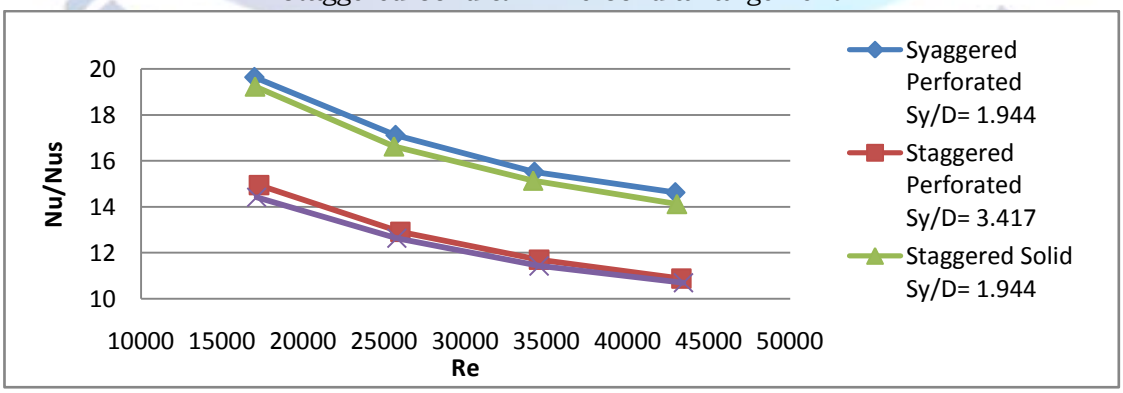

Fig:-4.3.3 Variation of Nu/Nus with Reynolds No. (Re) for various inter-fin spacing ratio (Sy/D) for Staggered ar

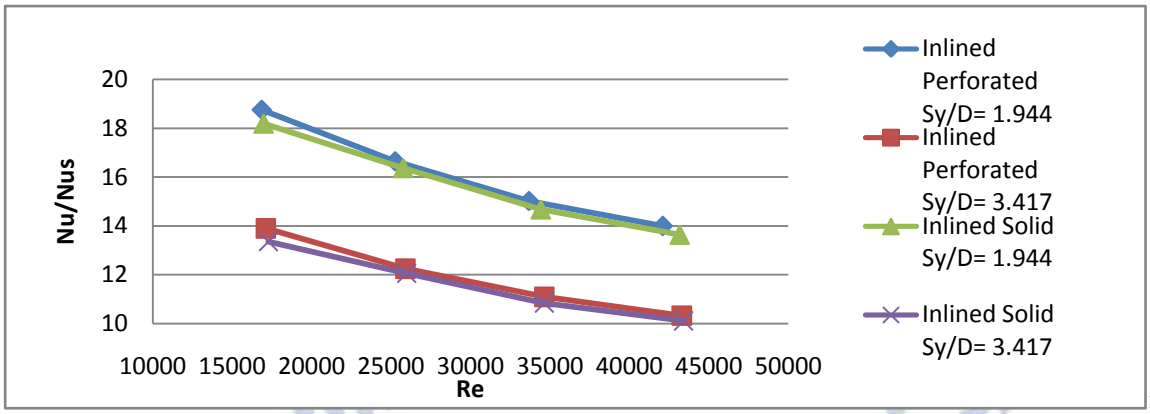

rangement

Fig:- 4.3.4Variation of Nu/Nus with Reynolds No. (Re) for various inter-fin spacing ratio (Sy/D) for Inline arrangement

Fig. 18 shows the behavior of the Nu/Nus as a function of the duct Reynolds number and inter-fin distance ratios (Sy/D) for a constant clearance ratio (C/H) of 0.0. Decreasing Sy/D means that the fin numbers on the base plate increases. It is seen from this figure that since the number of fins increases with decreasing

Sy/D, which also means an increase in the total heat transfer area, the heat transfer rate (Nu/Nus) increases. Perforated fins have higher Nusselt number values than solid fins.

Effect on Friction Factor

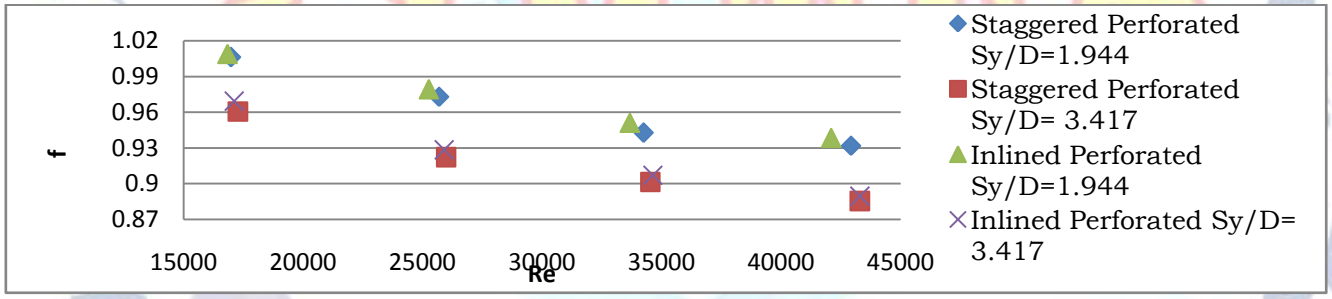

Fig:-4.37 Variation of Friction factor with Reynolds No. (Re) for various inter-fin spacing ratio (Sy/D) for Staggered Perforated & Inlined Perforated arrangements

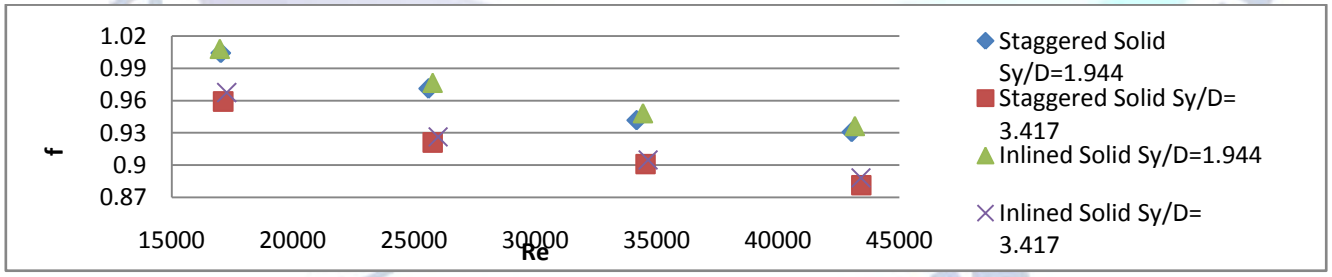

Fig:- 4.3.8Variation of Friction factor with Reynolds No. (Re) for various inter-fin spacing ratio (Sy/D) for Staggered Solid & Inlined Solid arrangement

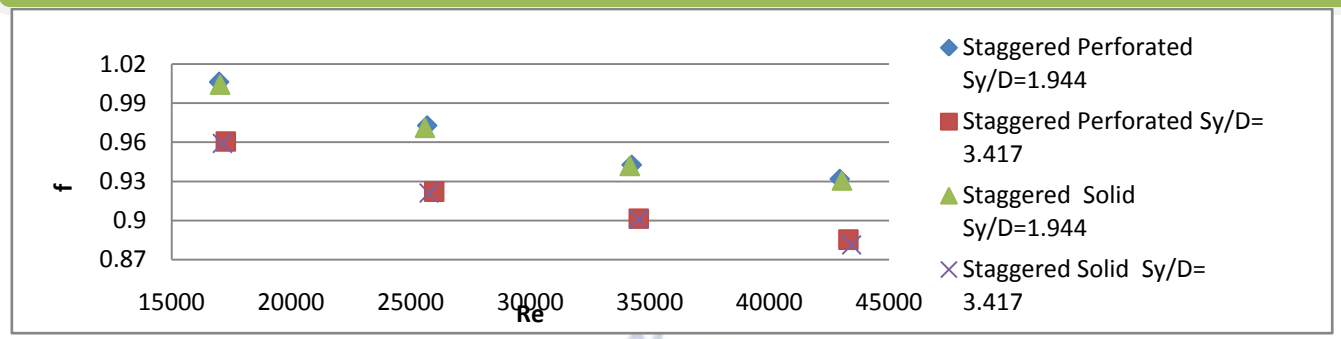

Fig:-4.3.9 Variation of Friction factor with Reynolds No. (Re) for various inter-fin spacing ratio (Sy/D) for Staggered arrangement

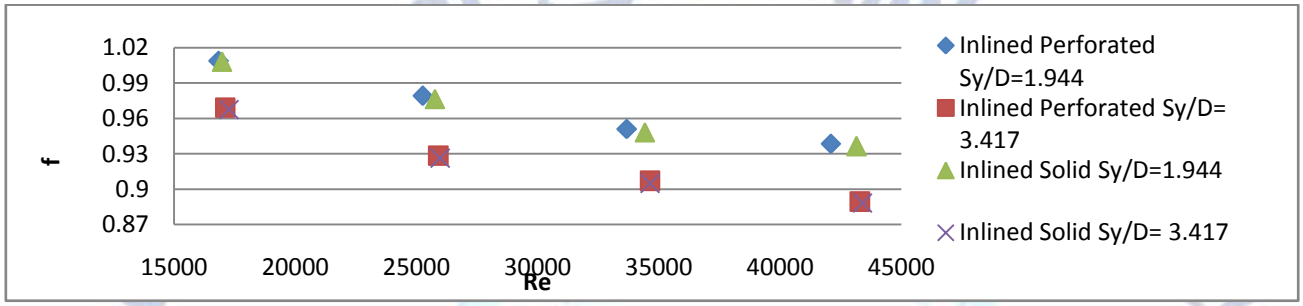

Fig:- 4.3.10 Variation of Friction factor with Reynolds No. (Re) for various inter-fin spacing ratio (Sy/D) for Inlined arrangement

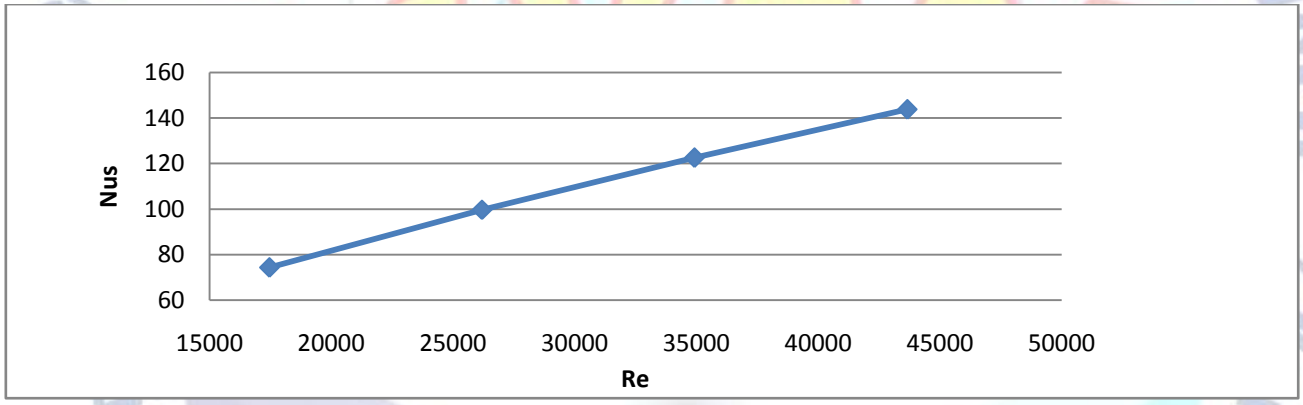

Fig:-4.3.11 Variation of Nu/Nus with Reynolds No. (Re) for various inter-fin spacing ratioSy/D) for Staggered Solid & Inline Solid arrangement

(a) The heat transfer enhancement efficiencies are higher than unity for all investigated conditions. This means that the use of pin fins leads to an advantage on the basis of heat transfer enhancement.
(b) Higher numbers of pin fins and longer pin fins have better performance. In other words, for higher thermal performance, a lower inter-fin distance ratio and clearance ratio should be preferred.
(c) At a lower Reynolds number, the channels with pin fin arrays give higher performance than those at a higher Reynolds number.

A.1 Heat Flow Pattern for Staggered Perforated Fins base plate with 4m/s velocity of fluid

1) 18 fins on base plate with 100mm height

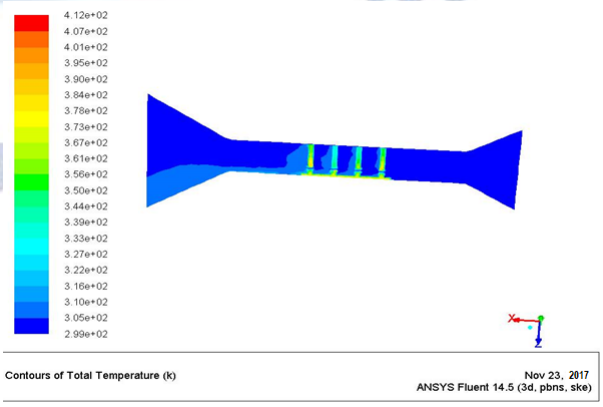

2) 11 fins on base plate with 100mm height

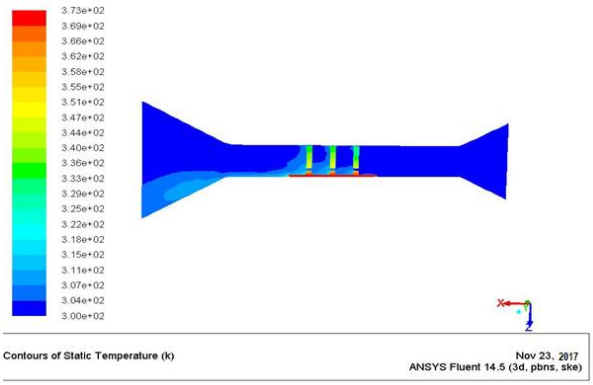

A.2 Heat Flow Pattern for Staggered Solid Fins Base plate with 4m/s velocity of fluid

1)18 fins on base plate with 100mm height

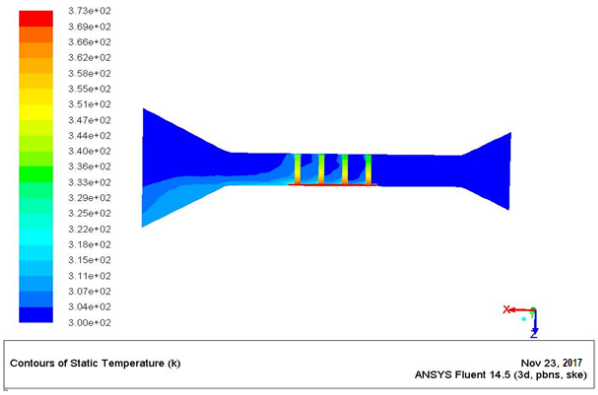

2)11 fins on base plate with 100mm height

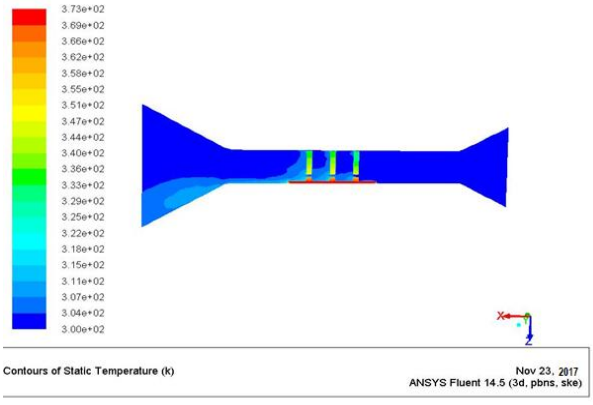

A.3 Heat Flow Pattern for Inline Perforated Fins base plate with 4m/s velocity of fluid

1) 35 fins on base plate with 100mm height.

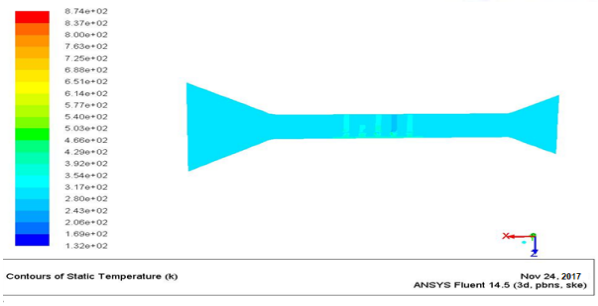

2) 21 fins on base plate with 100mm height

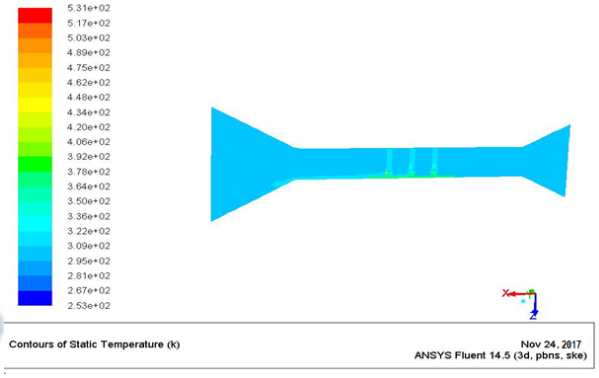

A.4 Heat Flow Pattern for Inline Solid Fins Base plate with 4m/s velocity of fluid

1)35 fins on base plate with 100mm height

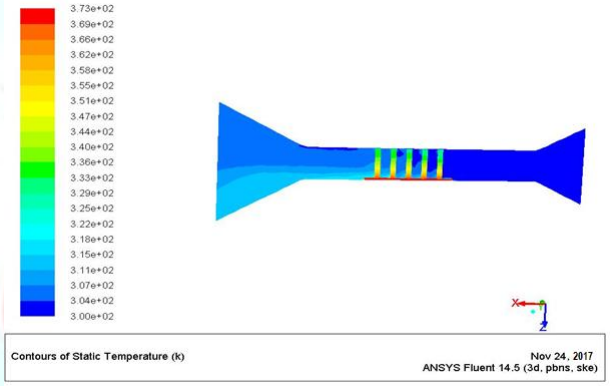

2) 21 fins on base plate with 100mm height

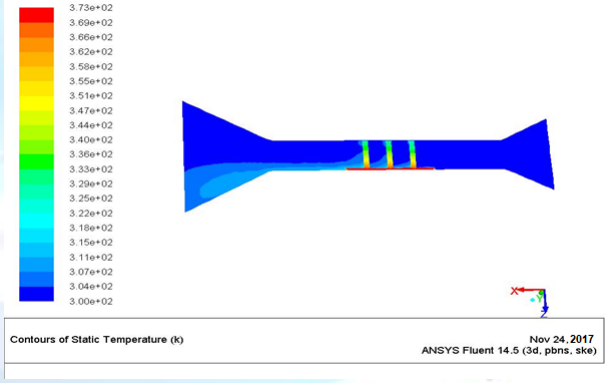

A.5 Heat Flow Pattern for Smooth base plate With 4m/s velocity of fluid

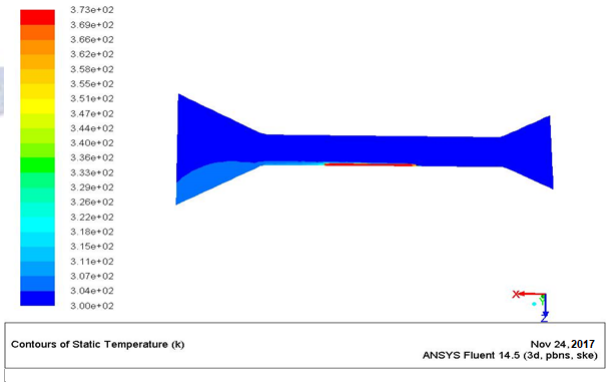

A.1 Heat Flow Pattern for Staggered Perforated Fins base plate with 5m/s velocity of fluid

1) 18 fins on base plate with 100mm height

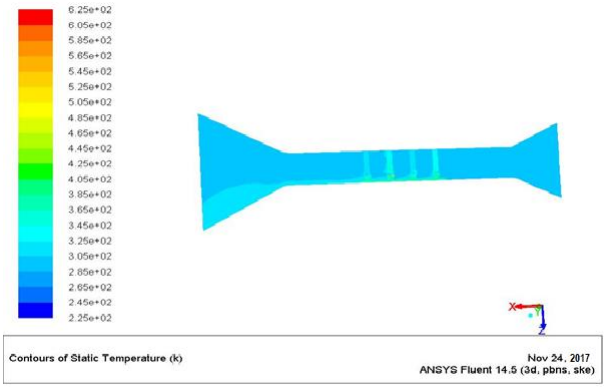

2) 11 fins on base plate with 100mm height

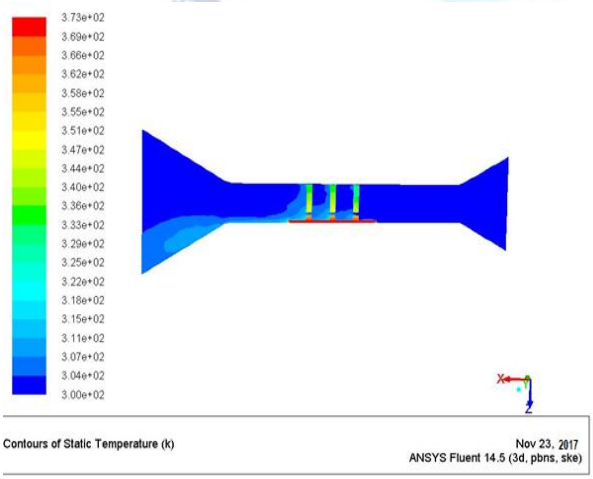

A.2 Heat Flow Pattern for Staggered Solid Fins base plate with 5m/s velocity of fluid

1) 18 fins on base plate with 100mm height

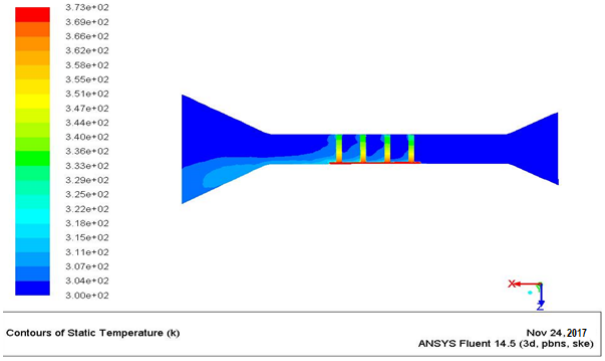

2)11 fins on base plate with 100mm height

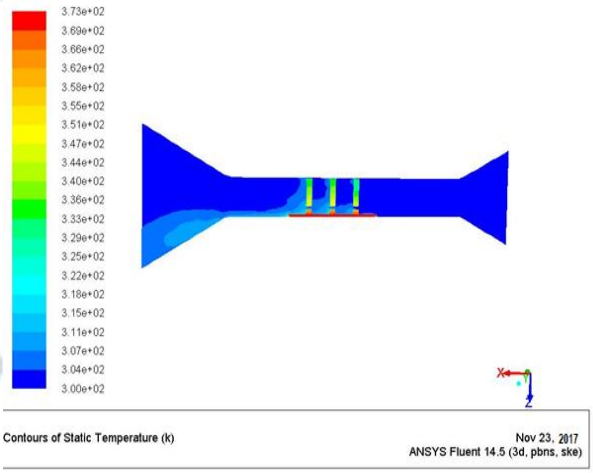

A.3 Heat Flow Pattern for Inline Perforated Fins base plate with 4m/s velocity of fluid

1) 35 fins on base plate with 100mm height.

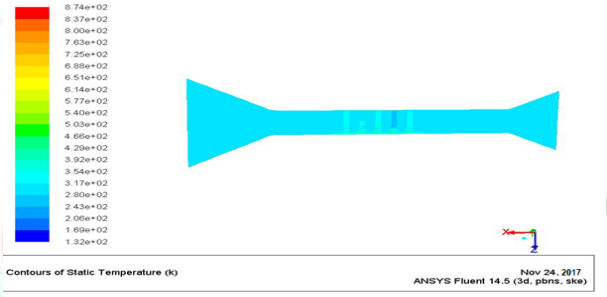

2) 21 fins on base plate with 100mm height

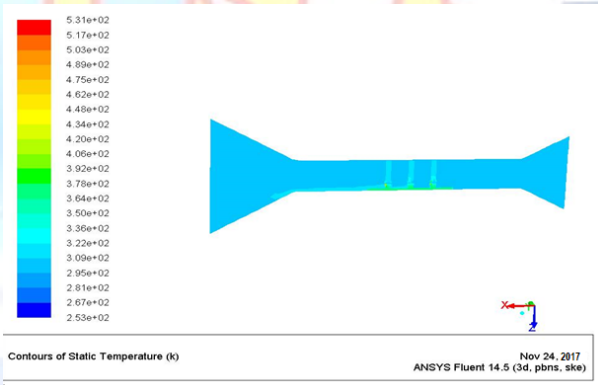

4 Heat Flow Pattern for Inline Solid Fins base plate with 4m/s velocity of fluid

1)35 fins on base plate with 100mm height

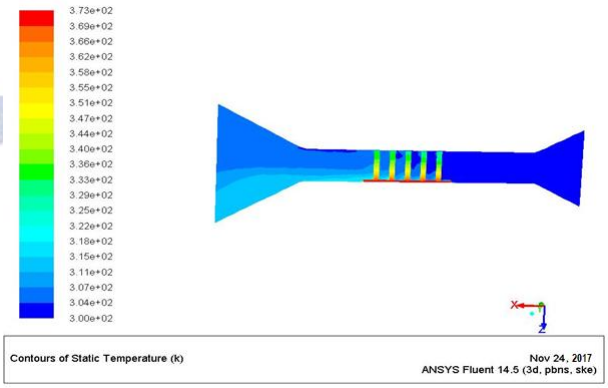

2) 21 fins on base plate with 100mm height

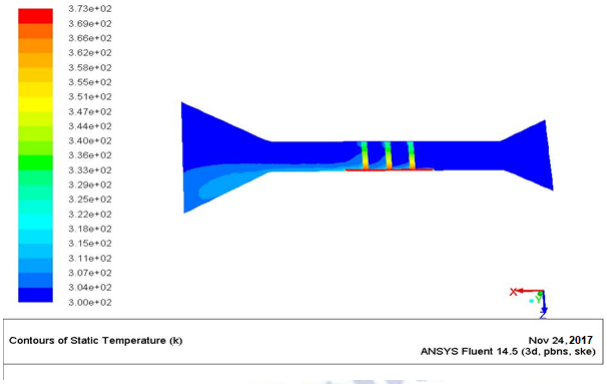

A.1 Heat Flow Pattern for Staggered Perforated Fins base plate with 5m/s velocity of fluid

1) 18 fins on base plate with 100mm height

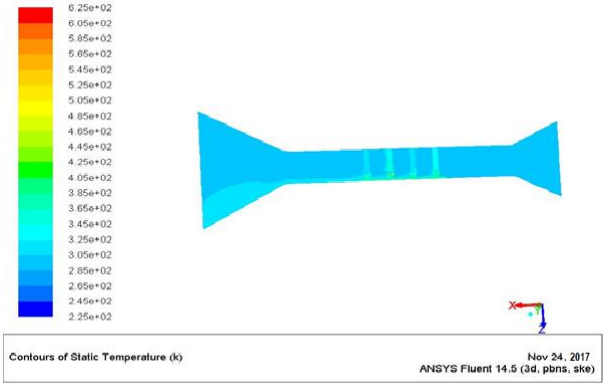

2) 11 fins on base plate with 100mm height

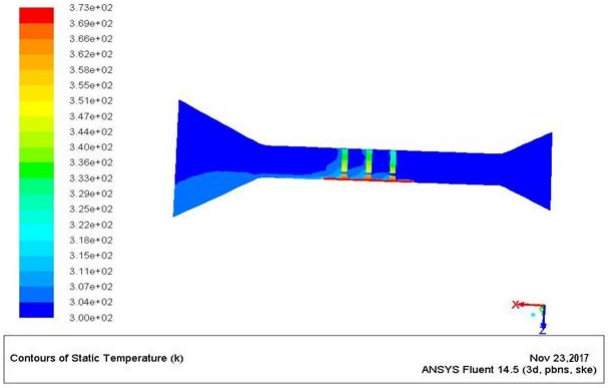

A.2 Heat Flow Pattern for Staggered Solid Fins base plate with 5m/s velocity of fluid

1) 18 fins on base plate with 100mm height

A.5 Heat Flow Pattern for Smooth base plate With 4m/s velocity of fluid

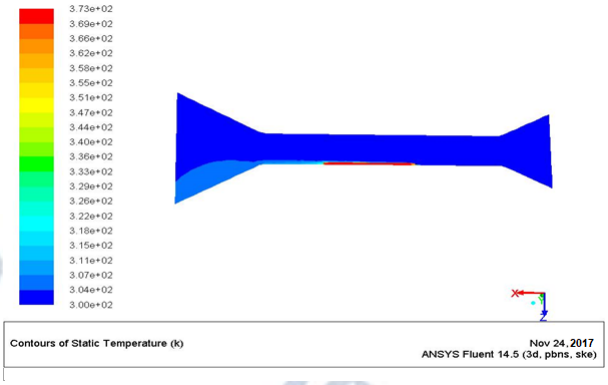

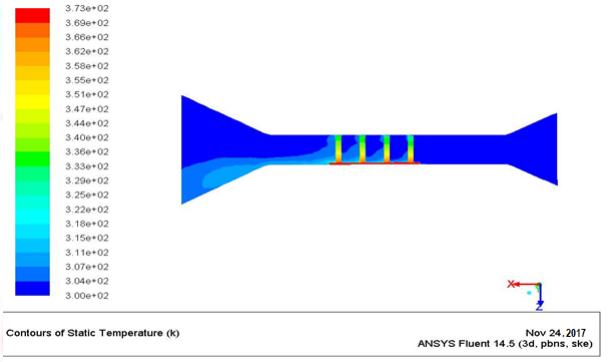

2) 11 fins on base plate with 100mm height

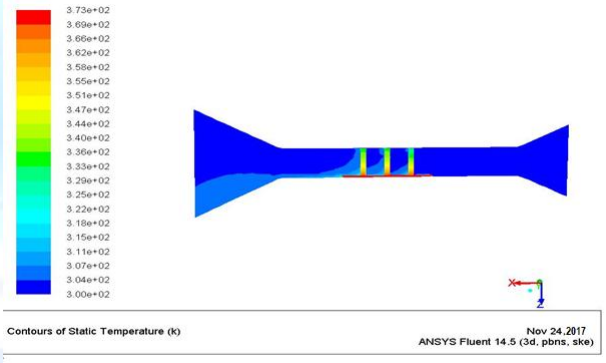

A.3 Heat Flow Pattern for Inline Perforated Fins base plate with 5m/s velocity of fluid

1) 35 fins on base plate with 100mm height

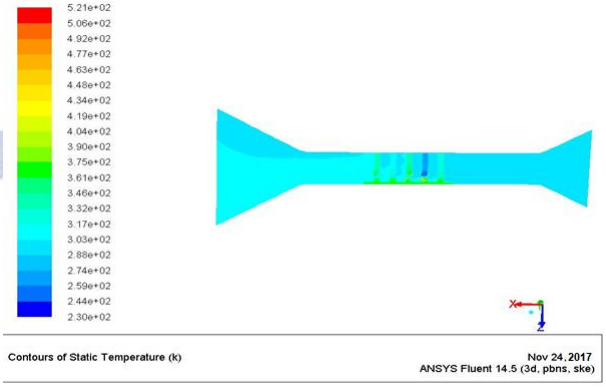

2) 21 fins on base plate with 100mm height.

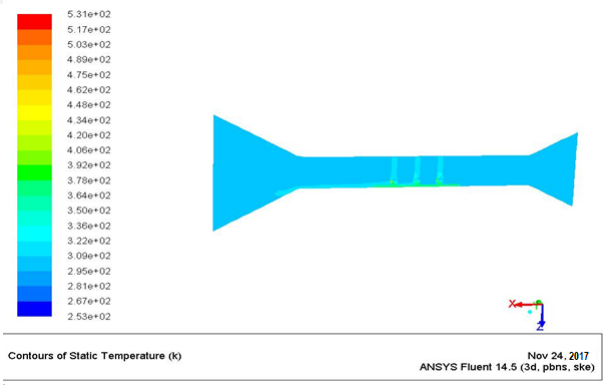

A.4 Heat Flow Pattern for Inline Solid Fins base plate with 5m/s velocity of fluid

1) 35 fins on base plate with 100mm height

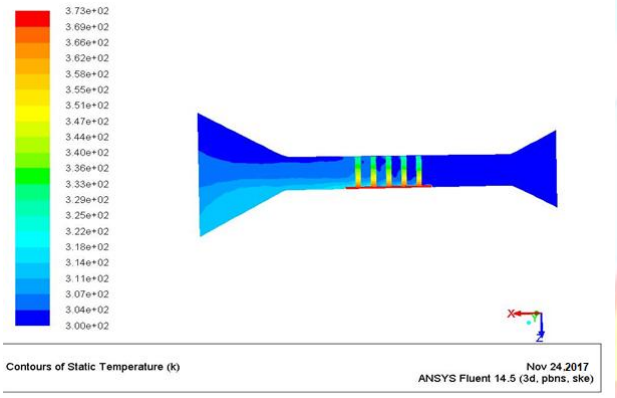

2) 21 fins on base plate with 100mm height

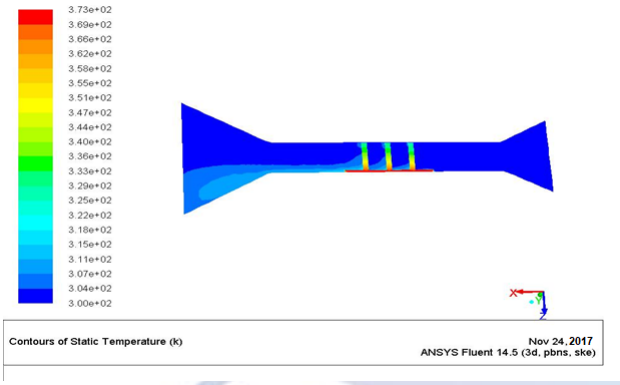

A.5 Heat Flow Pattern for Smooth base plate with 5m/s velocity of fluid

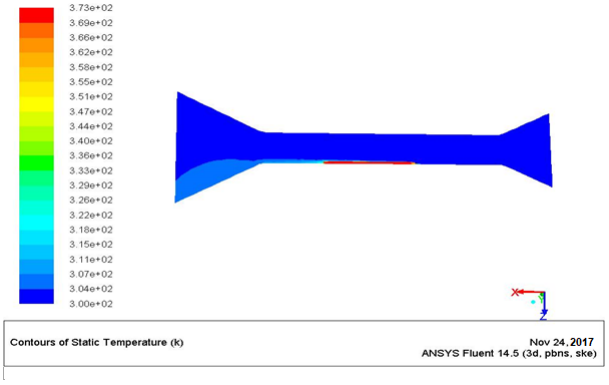

A.1 Air Flow Pattern for Staggered Perforated Fins base plate with 4m/s velocity of fluid

1) 18 fins on base plate with 100mm height

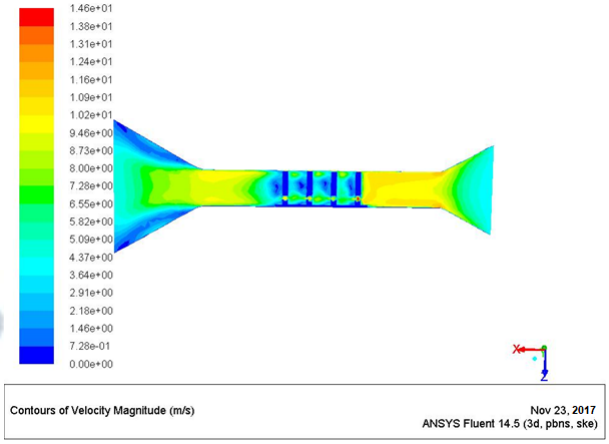

2) 11 fins on base plate with 100mm height

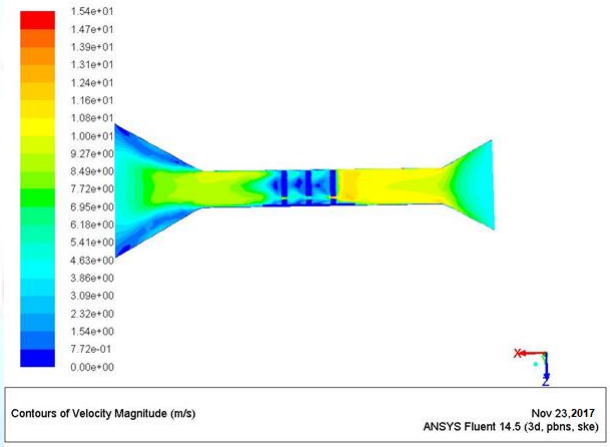

A.2 Air Flow Pattern for Staggered Solid Fins base plate with 4m/s velocity of fluid

1) 18 fins on base plate with 100mm height

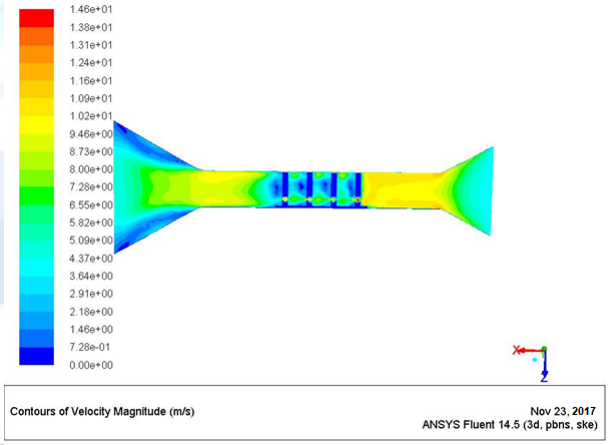

2) 11 fins on base plate with 100mm height

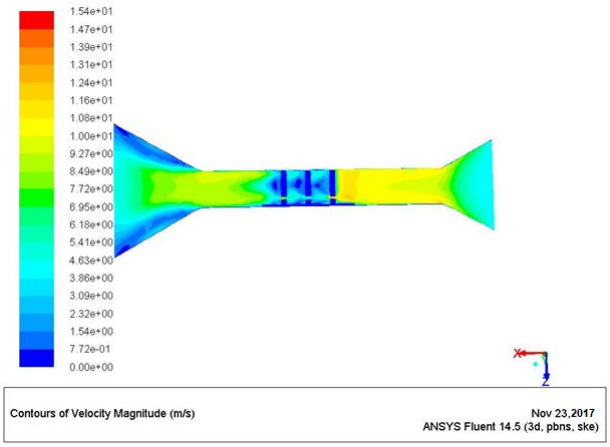

A.3 Air Flow Pattern for Inline Perforated Fins base plate with 4m/s velocity of fluid

1) 35 fins on base plate with 100mm height

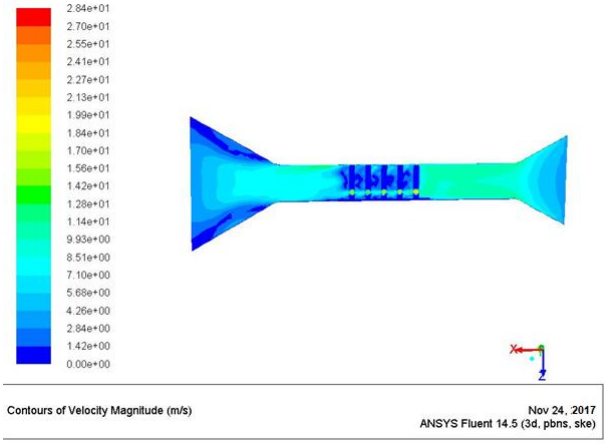

2) 21 fins on base plate with 100mm height

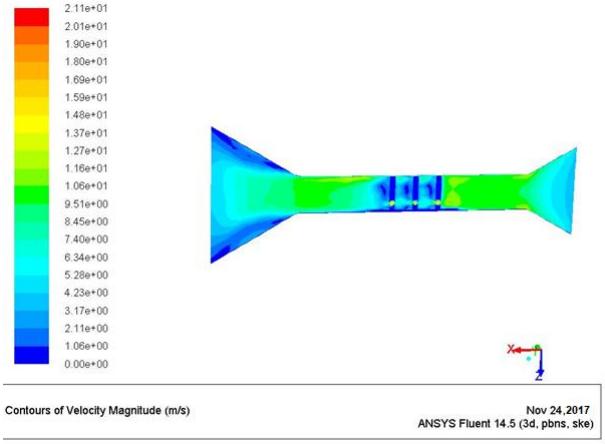

A.4 Air Flow Pattern for Inline Solid Fins base plate with 4m/s velocity of fluid

1) 35 fins on base plate with 100mm height

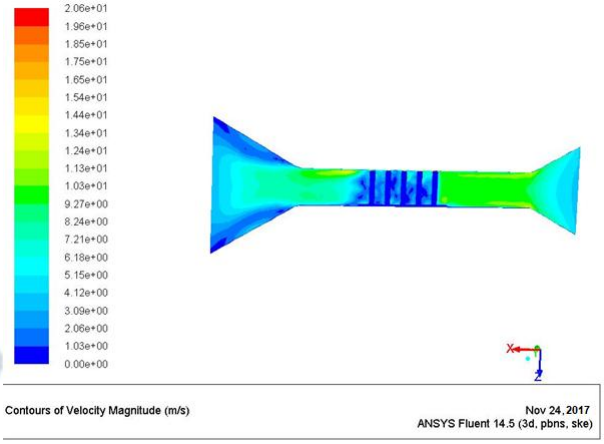

2) 21 fins on base plate with 100mm height

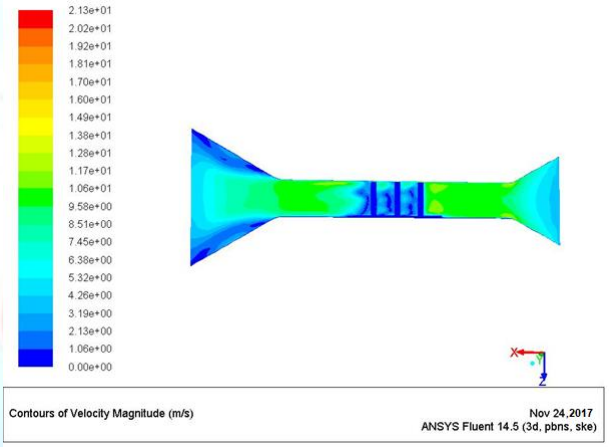

A.5 Air Flow Pattern for Smooth base plate with 4m/s velocity of fluid

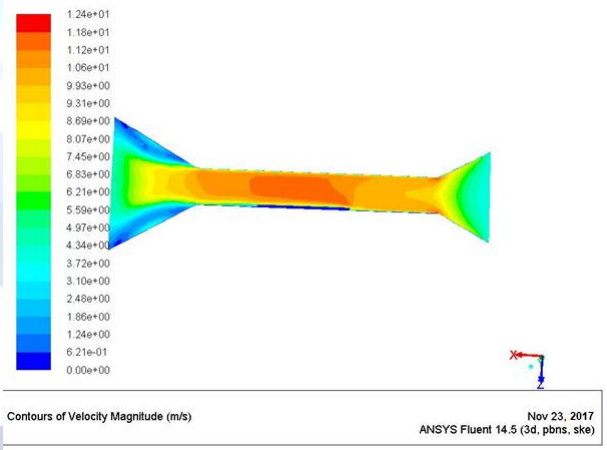

A.1 Air Flow Pattern for Staggered Perforated Fins base plate with 5m/s velocity of fluid

1) 18 fins on base plate with 100mm height

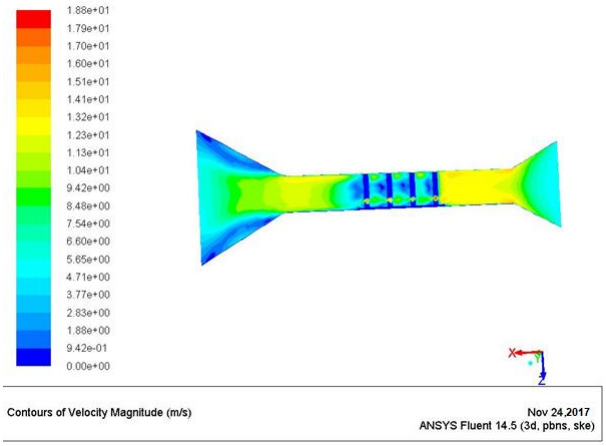

2) 11 fins on base plate with 100mm height

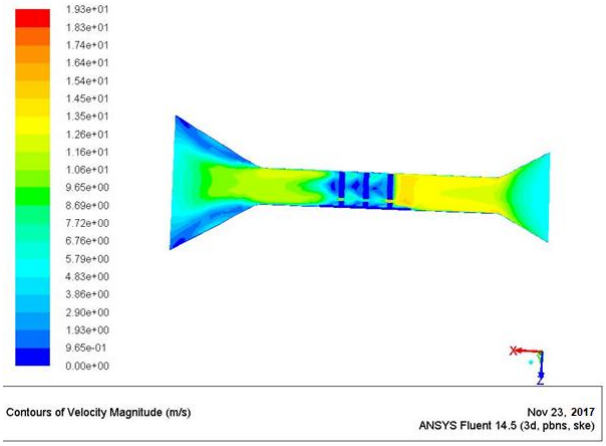

A.2 Air Flow Pattern for Staggered Solid Fins base plate with 5m/s velocity of fluid

1) 18 fins on base plate with 100mm height

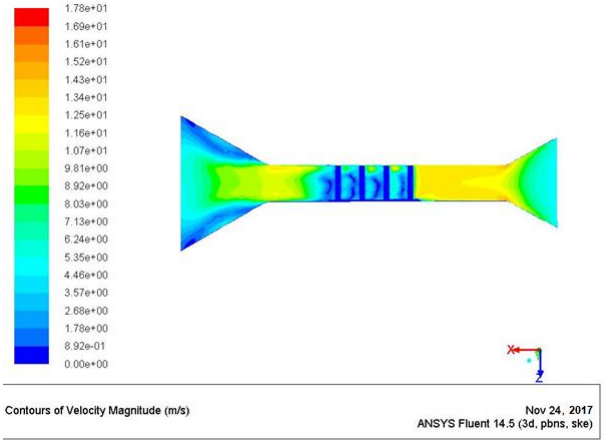

2) 11 fins on base plate with 100mm height

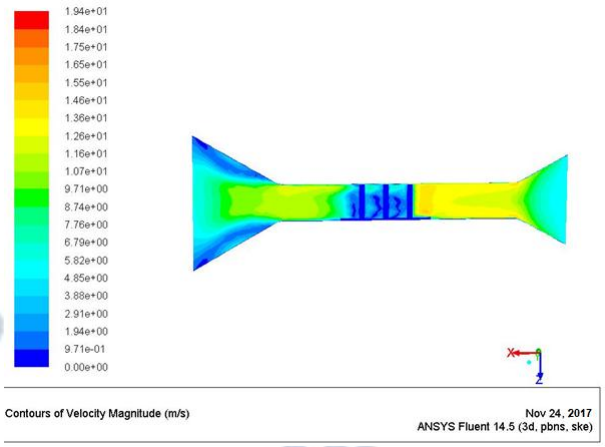

A.3 Air Flow Pattern for Inline Perforated Fins base plate with 5m/s velocity of fluid

1) 35 fins on base plate with 100mm height

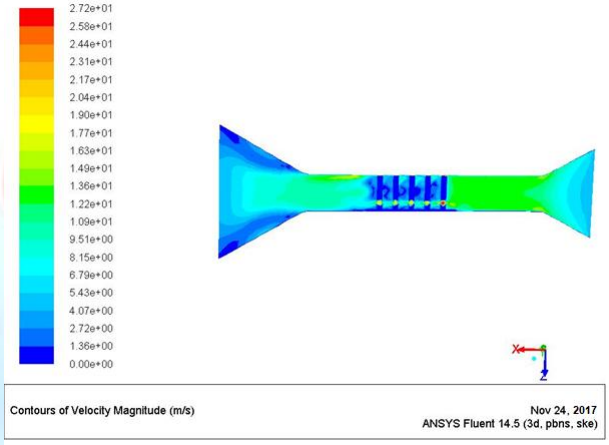

2) 21 fins on base plate with 100mm height

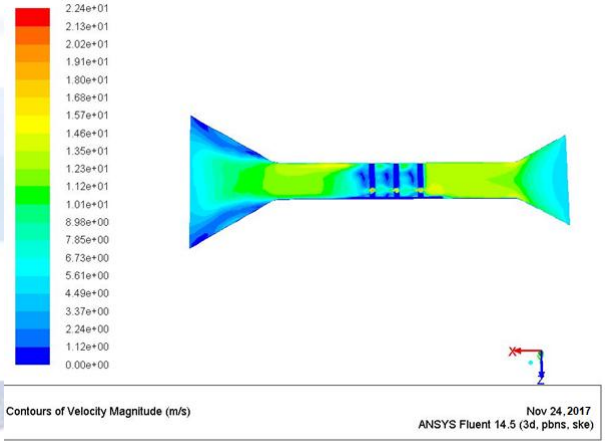

A.4 Air Flow Pattern for Inline Solid Fins base plate with 5m/s velocity of fluid

1) 35 fins on base plate with 100mm height

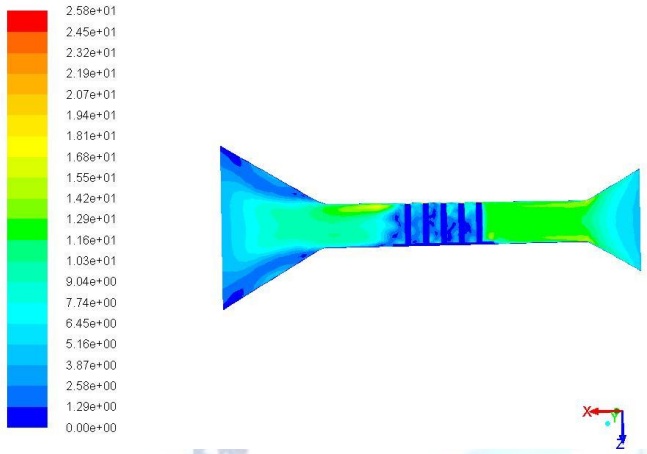

2) 21 fins on base plate with 100mm height

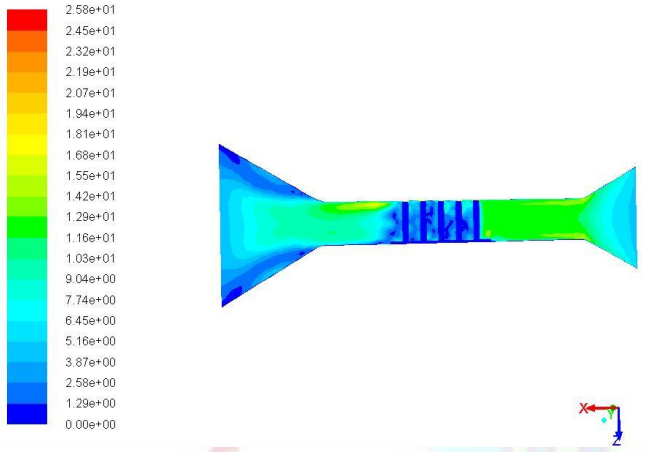

A.5 Air Flow Pattern for Smooth base plate with 5m/s velocity of fluid

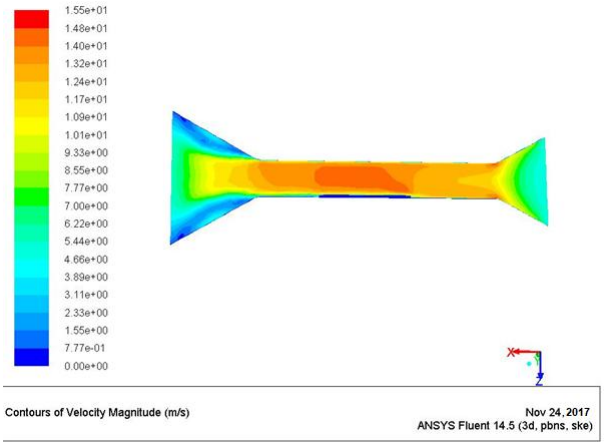

A.1 Temperature Variation across Base Plate for Staggered Perforated Fins with 4m/s velocity of fluid

1) 18 fins on base plate with 100mm height

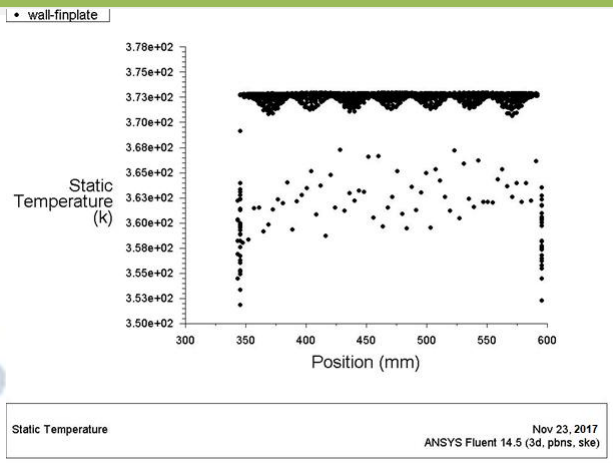

2) 11 fins on base plate with 100mm height

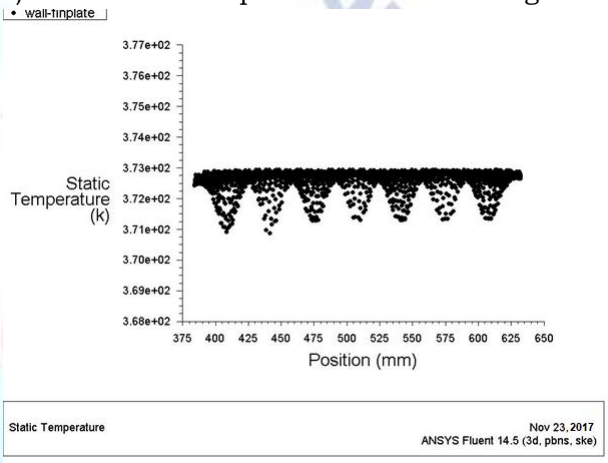

A.2 Temperature Variation across Base Plate for Staggered Solid Fins with 4m/s velocity of fluid

1) 18 fins on base plate with 100mm height

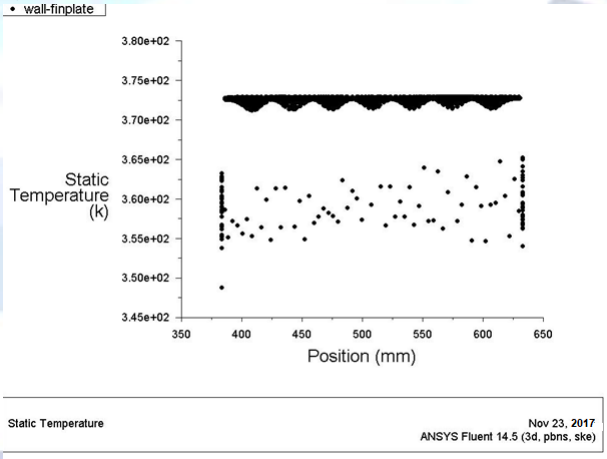

2) 11 fins on base plate with 100mm height

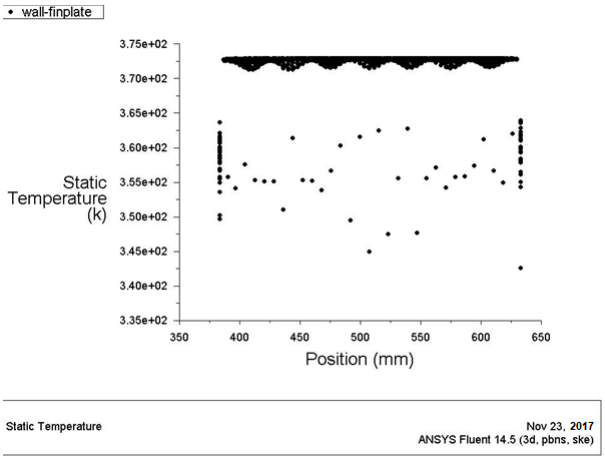

A.3 Temperature Variation across Base Plate for Inline Perforated Fins with 4m/s velocity of fluid

1)35 fins on base plate with 100mm height

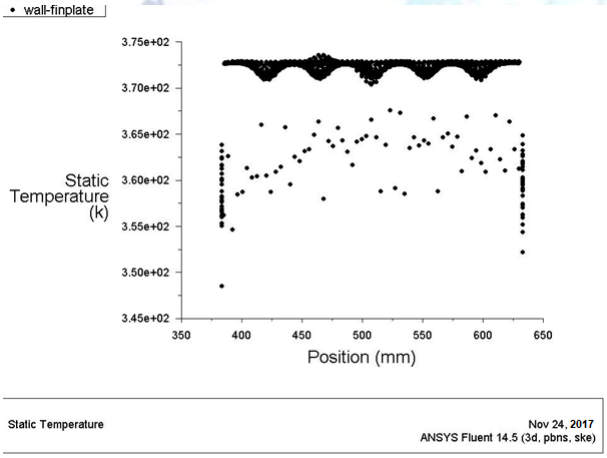

2) 21 fins on base plate with 100mm height

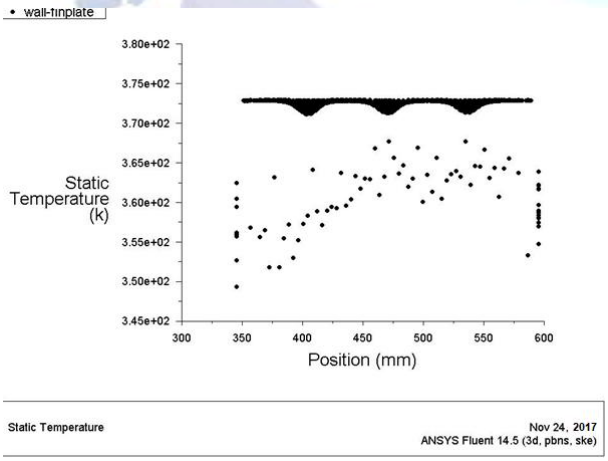

A.4 Temperature Variation across Base Plate for Inline Solid Fins with 4m/s velocity of fluid

1) 35 fins on base plate with 100mm height

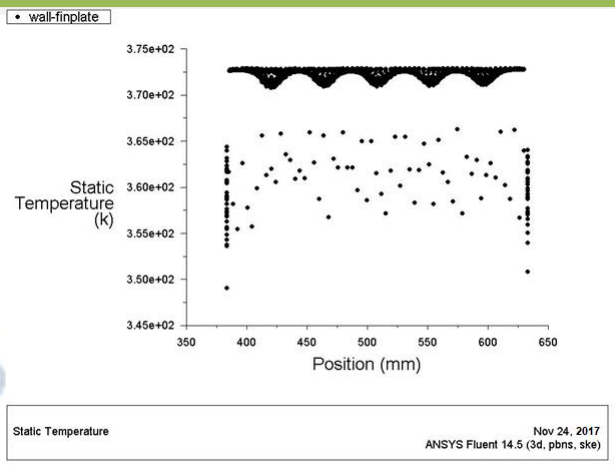

2) 21 fins on base plate with 100mm height

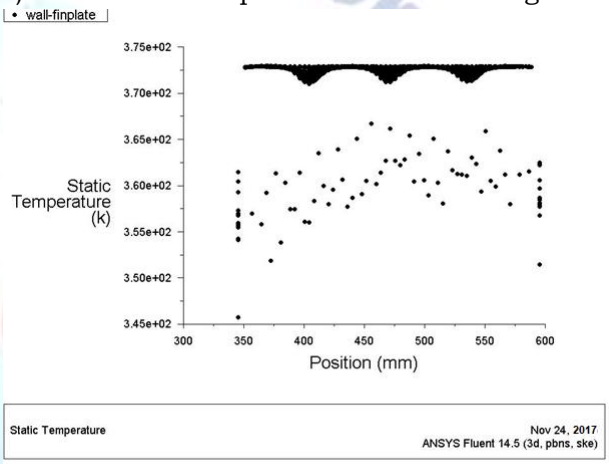

A.5 Temperature Variation across Smooth base plate with 4m/s velocity of fluid

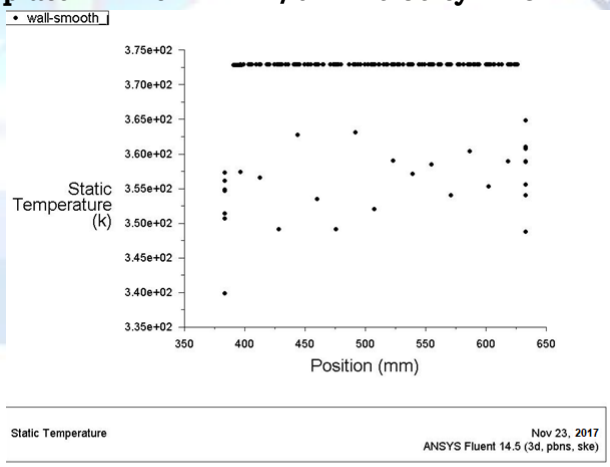

A.1 Temperature Variation across Base Plate for Staggered Perforated Fins with 5m/s velocity of fluid

1) 18 fins on base plate with 100mm height

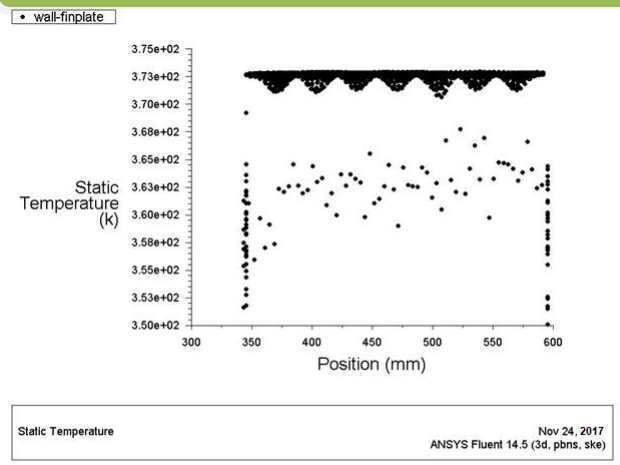

2) 11 fins on base plate with 100mm height

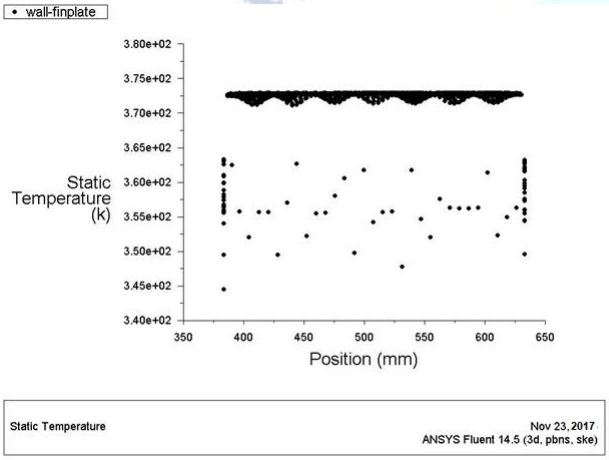

A.2 Temperature Variation across Base Plate for Staggered Solid Fins with 5m/s velocity of fluid

1) 18 fins on base plate with 100mm height

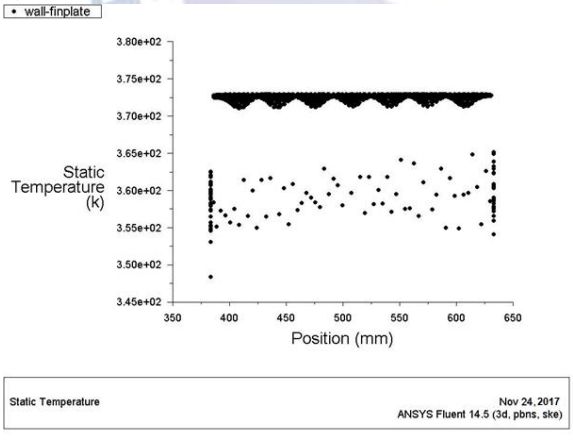

2) 11 fins on base plate with 100mm height

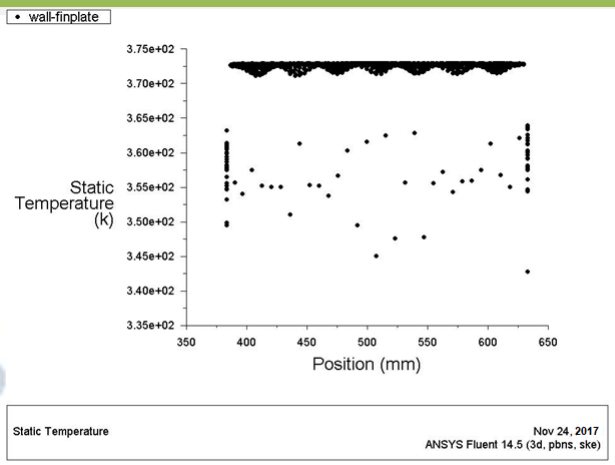

A.3 Temperature Variation across Base Plate for Inline Perforated Fins with 5m/s velocity of fluid

1) 35 fins on base plate with 100mm height

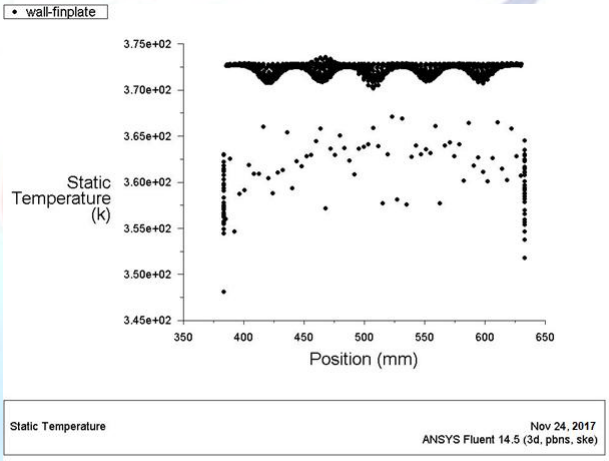

2) 21 fins on base plate with 100mm height

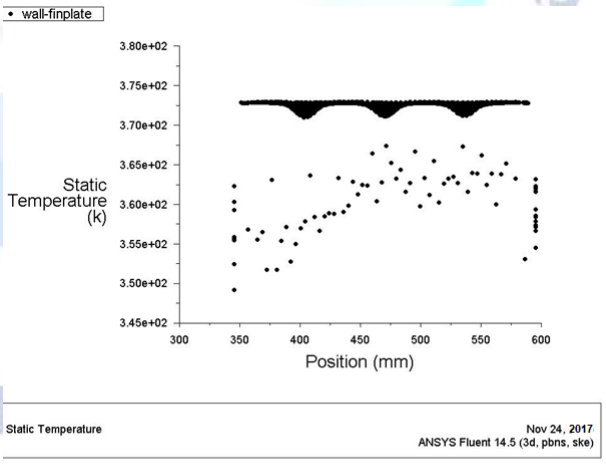

A.4 Temperature Variation across Base Plate for Inline Solid Fins with 5m/s velocity of fluid

1) 35 fins on base plate with 100mm height

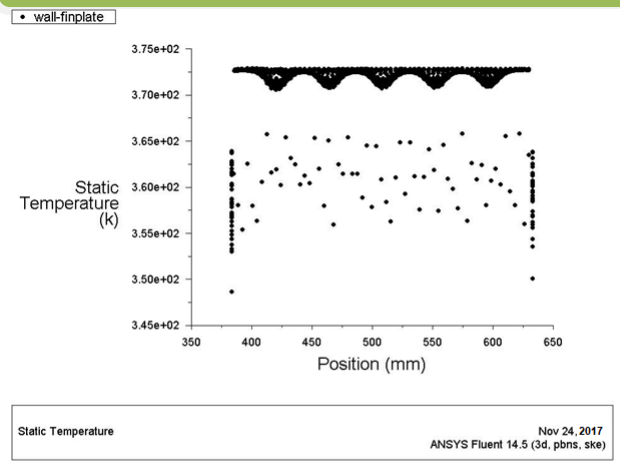

2) 21 fins on base plate with 100mm height

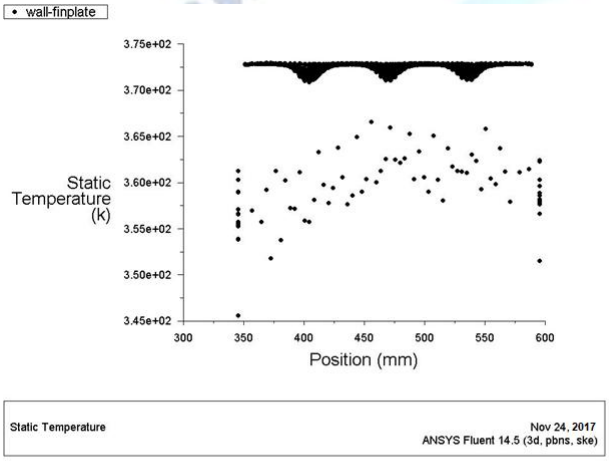

A.5 Temperature Variation across Smooth base plate
with 5m/s velocity of fluid

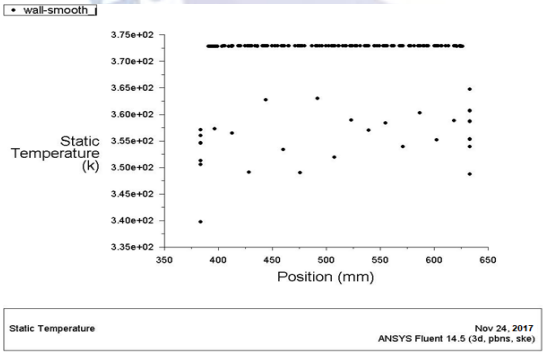

IV. CONCLUSION

In this study, the overall heat transfer, friction factor and the effect of the various design parameters on the heat transfer and friction factor for the heat experiment equipped with cylindrical cross-sectional perforated pin fins were investigated experimentally. The effects of the flow and geometrical parameters on the heat transfer and friction characteristics were determined, and the enhancement efficiency correlations have been obtained. The conclusions are summarized as:

(a) The average Nusselt number calculated on the basis of projected area increased with decreasing clearance ratio and inter-fin spacing ratio.

(b) The friction factor increased with decreasing clearance ratio and inter-fin distance ratio.

(c) Enhancement efficiencies increased with decreasing Reynolds number. Therefore, relatively lower Reynolds number led to an improvement in the heat transfer performance.

(d) The most important parameters affecting the heat transfer are the Reynolds number, fin spaces (pitch) and fin height. Heat transfer can be successfully improved by controlling these parameters. The maximum heat transfer rate was observed at 42,000 Reynolds number, 3.417 Sy/D and 50 mm fin height.

(e) The most effective parameter on the friction factor was found to be fin height. The minimum friction factor was observed at 50 mm fin height, 42,000 Reynolds number and 3.417 pitch

When all the goals were taken into account together, the trade-off among goals was considered and the optimum results were obtained at 42,000 Reynolds number, 50 mm fin height and 3.417 Sy/D pitch.

REFERENCES

[1] E.M. Sparrow, J.W. Ramsey, C.A.C. Altemani, Experiments on inline pin fin arrays and performance comparison with staggered arrays, Trans. ASME J. Heat Transfer 102 (1980) 44–50.

[2] G.J. Vanfossen and B.A. Brigham Length to diameter ratio and row number effects in short pin fin heat transfer, ASME J. Eng. Gas Turbines Power 106 (1984) 241–244.

[3] D.E. Metzger, C.S. Fan, S.W. Haley, Effects of pin shape and array orientation on heat transfer and pressure loss in pin fin arrays, J. Eng. Gas Turbines Power 106 (1984) 252–257.

[4] R. Karthikeyan* et al. / (IJAEST) International Journal of Advanced Engineering Science And Technology, Vol No. 10, Issue No. 1, 125 – 13

[5] O.N. Sara, T. Pekdemir, S. Yapici, M. Yılmaz, Heat-transfer enhancement in a channel flow with perforated rectangular blocks, Int. J. Heat Fluid Fl. 22, 509–518.

[6] M.K. Chyu, Heat transfer and pressure drop for short pin–fin arrays with pin–endwall fillet, ASME J. Heat Transfer 112 (9) (1990) 26– 32.

[7] S.C. Lau, J.C. Han, Y.S. Kim, Turbulent heat transfer and friction in pin fin channels with lateral flow ejection, ASME J. Heat Transfer 111 (1998) 51–58

[8] M. Tahat, Z.H. Kodah, B.A. Jarrah, S.D. Probert, Heat transfers from pin-fin arrays experiencing forced convection, Appl. Energy 67 (4) (2000) 419–442.

[9] K. Bilen, U. Akyol, S. Yapici, Heat transfer and friction correlations and thermal performance analysis for a finned surface, Energy Convers. Manage. 42 (2001) 1071–1083

[10] G. Tanda, Heat transfer and pressure drop in a rectangular channel with diamond-shaped elements, Int. J. Heat Mass Transfer 44 (2001) 3529–3541.

[11] J. P. Holman, 2004, "Heat Transfer", 9thEdition, Tata McGraw Hill Co," Pg. No. 43-53 & 315-350.

[12] Yunus A. Çengel, 2004, "Heat Transfer- A Practical Approach", SI units 2nd Edition, Tata McGraw Hill Co., Pg. No. : 156-168, 333-352 & 459-500.

[13] Tzer-Ming Jeng and Sheng-Chung-Tzeng ELSEVIER, International Journal of Heat and Mass Transfer 50 (2007) 2364–2375

[14] Bayram Sahim and Alparslan Demir Performance analysis of a heat exchanger having perforated square fins ,ELSEVIER, Applied Thermal Engineering 28 (2008) 621–632

[15] M. R.. Shaeri, M.and Yaghoubi. Numerical analysis of turbulent convection heat transfer from array of perforated fins. ELSEVIER International journal of heat and fluid flow 30 (2009) 218-228

[16] Jnana Ranjan Senapati and Sukanta Kumar Dash and Subhranshu Roy ,3D numerical study of the effect of eccentricity on heat transfer characteristics over horizontal cylinder fitted with annular fins. ELSEVIER International journal of Thermal Science.108 (2016)28-29

[17] Tamir K. Ibrahim,and Marwah N. Mohammed,and Mohammed kamil Mohammed,and Najafi,and Nor azwadi Che Sidik,and Firdaus Basrawi,and Ahamed n, Abdalla &and S.S. Hoseini . ELSEVIER International journal of Heat & Mass Transfer 118 (2018) 832-846